FACULTY OF ENGINEERING UNIVERSITY OF PORTO

Polysaccharide-based nanoparticles for cancer therapy

Inês Maria Pimentel Moreira

Porto, July 2012

Faculty of Engineering University of Porto

Polysaccharide-based nanoparticles for cancer therapy

Inês Maria Pimentel Moreira

Dissertation for the degree
Integrated Master in Bioengineering
Major: Biological Engineering
Supervisor: Prof. Dr. Maria do Carmo Pereira
Co-supervisor: Prof. Dr. Manuel Coelho

July 2012

“Learn from yesterday, live for today, hope for tomorrow.
The important thing is to not stop questioning.”

Albert Einstein

Acknowledgments

There are numerous people that, directly or indirectly, contributed to the development of this work and to whom I have to thank so much.

First of all, I would like to thank my supervisor, Prof. Maria do Carmo Pereira, for her valuable and constant advice, corrections and kindness. I am grateful to my co-supervisor Prof. Manuel Coelho and also Dr. Sandra Rocha, for the comments and suggestions.

I have to thank my colleagues from the lab 204A, Diana, Joana and Sílvia for their essential help and fellowship, and in special to Manuela, for her priceless help on the cytotoxicity studies, and to Mireia, for the important work discussions and company.

I also would like to thank technicians of DEQ for their kindness, Rui Fernandes from IBMC for the TEM morphologic analysis and Dr. Filipe Santos Silva (Tumor Molecular Models Group) and Dr. Gabriela M. Almeida (Cancer Drug Resistance Group) from IPATIMUP, for kindly providing the human pancreatic cancer cell line (provided by Prof. M. A. Hollingsworth, UNMC – Omaha, USA), as well as all the materials and facilities necessary for developing the cytotoxicity studies.

To my colleagues and friends Ana Luísa, Catarina, João Pedro, Maria do Carmo, Ana Catarina, Carolinas, Diogo, Francisco and Soraia, thanks for the company at lunch and free time, as well as for the numerous conversations and encouragement words.

Thank you to my other friends, for understanding my absence and for the quality time spent together.

Last but not least, I am totally grateful to my family, especially my parents and sister Rita, for their continuous support, encouragement and for being my model to follow. And to Nuno, for his constant presence and for providing me good moments.

Abstract

New strategies for anticancer drug delivery ought to be developed in order to overcome the limitations and the harmful side effects of conventional cancer treatments. Nanoparticles, and in particular polysaccharide-based ones, are being extensively investigated as carriers for the delivery of chemotherapeutic agents, enhancing their blood circulation time and, thus, increasing therapeutic efficiency. In this work, two chitosan-based nanocarriers were produced by ionic gelation with tripolyphosphate and gum arabic for the encapsulation of the anticancer drug gemcitabine and its delivery into pancreatic tumour cells. The parameters that significantly influenced the nanoparticle formulation were the chitosan molecular weight, polymers concentration and mass concentration ratio. The produced nanoparticles were within the size range of 200-400 nm, presenting a low polydispersity index, a positive zeta potential and a spherical shape. The chitosan/gum arabic nanoparticles presented a more adequate behaviour than chitosan/tripolyphosphate, having attained a medium gemcitabine encapsulation efficiency of 38%, a loading capacity of 10% and a process yield of approximately 50%. The encapsulation efficiency and the drug loading were significantly increased when the nanoparticles were coated with polysorbate 80, that acted as a stabilizing agent. Studies on the drug release from the chitosan/gum arabic nanoparticles have shown a biphasic pattern with a burst initial release, attributed to the free and adsorbed drug, followed by a slower controlled release, correspondent to the entrapped gemcitabine inside the core of the nanoparticles. The *in vitro* cytotoxic effects on a pancreatic cancer cell line upon treatment with gemcitabine-loaded chitosan/gum arabic nanoparticles were assessed. These gemcitabine-loaded nanocarriers have shown to have cytotoxic effect on this pancreatic tumour cell, although it took a longer time for gemcitabine in the nanoparticles to decrease cell survival and inhibit cell growth than for free gemcitabine. From this work, it is possible to conclude that chitosan/gum arabic-gemcitabine nanosystem is a promising alternative for the gemcitabine controlled release into tumour cells, since it increases gemcitabine half-life and consequently enhances its therapeutic efficiency.

Keywords: Nanocarriers, Polysaccharides, Pancreatic cancer treatment, Tumour targeting, Controlled delivery, Therapeutic efficiency, Cytotoxicity effect

Contents

List of Figures

List of Tables

List of Abbreviations

CS: Chitosan

D: Diffusion coefficient

DD: Degree of deacetylation

DLS: Dynamic light scattering

DOX: Doxorubicin

DSC: Differential scanning calorimetry

df: degrees of freedom

d_p: Hydrodynamic diameter

EE: Encapsulation efficiency

EPR: Enhanced permeability and retention

FDA: Food and Drug Administration

FTIR: Fourier Transform Infrared spectroscopy

$f(k_a)$: Henry's function

GA: Gum Arabic

Gem: Gemcitabine

GI_{50}: Half maximal growth inhibitory concentration

HER2: Human epidermal growth factor receptor 2

IC_{50}: Half maximal inhibitory concentration

η: Viscosity

K_B: Boltzmann constant

LC: Loading capacity

LMWC: Low molecular weigth chitosan

MMWC: Medium molecular weigth chitosan

MPS: Monocyte phagocytosis system

MW: Molecular weight

MWCO: Molecular weight cut off

NMR: Nuclear magnetic resonance spectroscopy

NPs: Nanoparticles

PB: PrestoBlue

PBS: Phosphate buffered saline

PdI: Polydispersity index

PEC: Polyelectrolyte complexation

PEG: Polyethylene glycol

PF127: Pluronic F-127

PTX: Paclitaxel

p80: Polysorbate 80

SD: Standard deviation

SEM: Standard error of the mean

SNP: Self-assembled nanoparticles

SRB: Sulforhodamine B

T: Temperature

TEM: Transmission electron microscopy

TPP: Pentasodium tripolyphosphate

U_E: Electrophoretic mobility

ζ / ZP: Zeta potential

1 Introduction

1.1 Motivation

Cancer remains one of the world's major causes of death and the improvement of its effective therapies is a continuous challenge for researchers. The main problems of the actual chemotherapeutic treatments are related with the toxicity caused by the anticancer drugs on normal tissues, since they present poor biopharmaceutical properties and are nonspecific to the tumour cells. This issue leads to a higher administered drug need, and all these factors together cause several harmful side effects in patients.

These limitations are recently leading to numerous investigations in order to design and develop an ideal formulation for the anticancer drug specific and controlled release. In fact, there has been a growing realization that an ideal anticancer nanocarrier can and must be carefully engineered, in what matters to size, shape and surface, according to the type, stage and location of the cancer in question. Polymers, and in particular polysaccharides, are being studied and employed in the production of nanoparticles able to deliver anticancer drugs, due to their favourable physical and biological properties. There is a belief that this technology will be, in the future, very important for clinical and biomedical applications in cancer therapy and imaging.

1.2 Main objectives

The aim of this work is to develop nanosystems capable of encapsulating an anticancer drug and delivering it to specific tumour cells, significantly reducing toxic side effects. The first step is to produce chitosan/tripolyphosphate (CS/TPP) and chitosan/gum arabic (CS/GA) nanoparticles by ionic gelation method, using the ionic crosslinking between TPP and chitosan, and the electrostatic interactions between chitosan and gum arabic, respectively, and characterize them. Consequently, the gemcitabine-loaded nanoparticles (NPs) are also

characterized and evaluated as nanocarriers of gemcitabine for its delivery into pancreatic cancer cells.

Some studies on the preparation of chitosan nanoparticles by ionic gelation with TPP to deliver gemcitabine have been recently published. However, to our knowledge, any study was developed on gemcitabine-loaded nanoparticles using the electrostatic interaction between the polysaccharides chitosan and gum arabic for its controlled release into cancer cells.

1.3 Thesis organization

This thesis is divided in 6 chapters.

Chapter 1 focus on the main motivations to design and develop anticancer drug nanocarriers based on polysaccharide nanoparticles. Additionally, the main objectives of this work are defined.

Chapter 2 presents the state of the art at this moment, it means, the studies that have been developed so far on the anticancer drug delivery using nanoparticles, in particular the polysaccharide-based ones.

The most important materials, reagents and methods used throughout the work are presented on Chapter 3.

On Chapter 4, the principal obtained results and respective discussion for the CS/TPP nanoparticles characterization and evaluation are shown, being the ones relative to the CS/GA system analysed and discussed on Chapter 5.

The overview of this study, its main conclusions and some future work perspectives are presented on Chapter 6.

2 State of the Art

2.1 Cancer therapy problematic

The first problem associated with chemotherapy in cancer therapy is the fact that the used anticancer drugs are largely toxic and poorly soluble (Feng and Chien, 2003; Qiao *et al.*, 2010). Furthermore, it has been realized during the past few decades that most conventional chemotherapeutic drugs for cancer therapy lack on specificity, being not able to distinguish between cancerous and normal cells (Gu *et al.*, 2007; Nie *et al.*, 2007). Besides, as the delivery system is not selective and the effective concentration of the medicine in the tumour cells is lower than expected, a larger quantity of drug administered is required (Sinha *et al.*, 2006), which is not economical and usually leads to unwanted toxic side effects (Na *et al.*, 2003; Cho *et al.*, 2008). These are the reasons why there is a limited maximum allowable dose (Sinha *et al.*, 2006; Nie *et al.*, 2007). Accordingly, researchers are seeking to attain new therapeutic strategies and formulations such as drugs' carriers in order to overcome these limitations (Park *et al.*, 2008; Qiao *et al.*, 2010).

2.2 Nanoparticles as anticancer drug carriers

In recent years, a growing number of studies focused on the research and development of nanoparticles capable of carrying chemotherapeutic drugs within and control-releasing it when bound to the specific tumour tissue has been published (Gu *et al.*, 2007; Peer *et al.*, 2007). The main advantages of using nanoparticles as drug delivery systems are related with their small size and use of biodegradable materials (Singh and Lillard, 2009): a) they can pass through the smallest capillary vessels (Liu *et al.*, 2008); b) they can guide drugs more precisely to tumour cells and reduce toxic side effects (Duncan, 2006; Liu *et al.*, 2008; Shi *et al.*, 2011);

c) they present the ability to deliver drugs at the therapeutic concentration to multiple areas for long periods of time (Hans and Lowman, 2002); d) they present an improved solubility (Singh and Lillard, 2009); among many others.

The tumour cells obtain nutrients by passive diffusion and continually grow by forming new blood vessels (angiogenesis) to supply nutrients and oxygen to the increasing mass (Haley and Frenkel, 2008). This rapid vascularisation results in a high tortuosity and defective vascular structure and in a low lymphatic drainage, making it possible for the passive drug targeting to take advantage of the tumour environment via the leaky vessels (Sinha *et al.*, 2006; Park *et al.*, 2008) (Figure 1). Besides, this structure allows an enhanced permeability and retention (EPR) effect that allows the accumulation of nanoparticles at the tumour site (Nie *et al.*, 2007; Malam *et al.*, 2009).

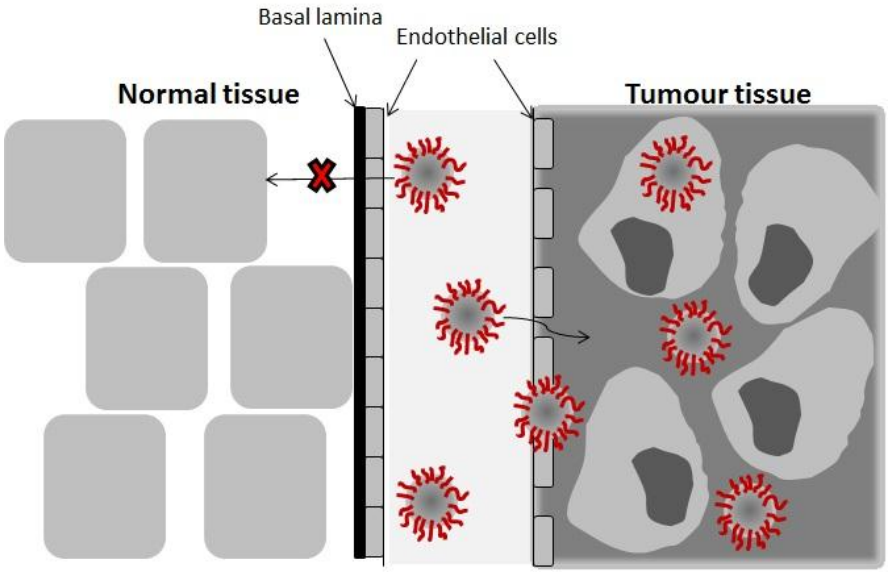

Figure 1 – Schematic diagram showing enhanced permeability and retention (EPR) effect in tumour tissues, in comparison to the occurred in normal tissues.

In addition to their size, the surface characteristics of nanoparticles are also an important factor that can be customized to avoid capture by macrophages that are fixed in the reticuloendothelial system (Cho *et al.*, 2008). To ensure that the nanoparticles escape macrophage uptake and are not adsorbed by plasma proteins, they should have a hydrophilic surface, which is normally achieved by coating their surface with a biodegradable copolymer with hydrophilic characteristics such as polyethylene glycol (PEG), procedure named PEGylation (Nie *et al.*, 2007; Cho *et al.*, 2008; Singh and Lillard, 2009).

However, it is predictable that a drug delivery system that depends only on passive targeting mechanisms is specificity-limited (Cho *et al.*, 2008) since some tumours lack of the EPR effect, and it is difficult to control such a random process (Peer *et al.*, 2007). In order to overcome these limitations, one approach was suggested: the inclusion of a targeting ligand or antibody in the polymer-drug binary conjugates, that binds with high affinity to the tumour cell

surface receptors or antigens, respectively (Sinha *et al.*, 2006; Cho *et al.*, 2008). This mechanism is termed active targeting and is able to provide preferential accumulation of the drug in the tumour zone (Sinha *et al.*, 2006; Nie *et al.*, 2007) (Figure 2).

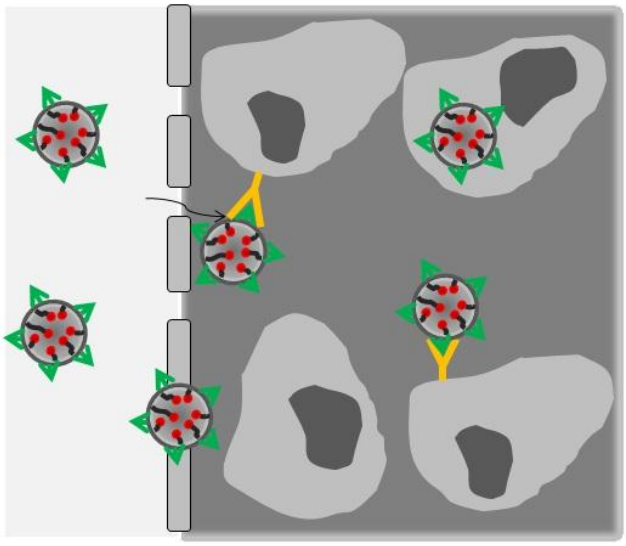

Figure 2 - Schematic diagram showing active targeting using targeting ligands in tumour tissues.

These nanometre-sized particles (10^{-9} metres) as medicine carriers are being engineered and constructed both for already existing and new drugs (Haley and Frenkel, 2008). Despite the extensive investigation and development in the field of nanoparticles as drug carriers, only a few are currently approved by the Food and Drug Administration (FDA) and available for cancer treatment (Haley and Frenkel, 2008). The first ones to be approved were liposomal formulations, the pegylated liposomal doxorubicin (Doxil® or Caelyx®, varying from the U.S. to outside the U.S., respectively) and daunorubicin citrate liposome injection (DaunoXome®) (Duncan, 2006; Haley and Frenkel, 2008). Most recently, in 2005, Abraxane®, albumin-entrapped paclitaxel nanoparticles, has been approved for the treatment of breast cancer (Duncan, 2006; Haley and Frenkel, 2008).

According to structural characteristics, the most known methodologies for the preparation of nanoparticles are the covalent crosslinking and ionic crosslinking, as well as polyelectrolyte complexation and self-assembly of hydrophobically modified polysaccharides (Liu *et al.*, 2008). However, before the decision of which of the synthesizing techniques to use, the nature of the drug, the drug carrier and the means and time desired for the delivery must be taken into account (Hans and Lowman, 2002). Natural and synthetic polymers, lipids and inorganic materials are typically used as drug delivery vectors (Peer *et al.*, 2007).

2.3 Polysaccharide-based nanoparticles

Biocompatibility, biodegradability and stability are the basic characteristics of polymers used as biomaterials to the preparation of nanoparticles for controlled release (Yang *et al.*, 2006; Peer *et al.*, 2007; Singh and Lillard, 2009). As natural polymers, polysaccharides follow these expectations, other than being safe and non-toxic (Lemarchand *et al.*, 2004; Liu *et al.*, 2008).

In fact, several polysaccharides have been highly studied as carriers for the controlled drug release (Sinha and Kumria, 2001; Trickler *et al.*, 2010; Wilson *et al.*, 2010), as agents for imaging application (Saravanakumar *et al.*, 2009; Barreto *et al.*, 2011), among several others (Janes *et al.*, 2001; Yoo *et al.*, 2005). In order to attain these purposes, polysaccharides can be used either to prepare nanoparticles (Kwon *et al.*, 2003; Na *et al.*, 2003; Yoo *et al.*, 2005; Zhang *et al.*, 2007; Al-Qadi *et al.*, 2011), as coating materials (Lemarchand *et al.*, 2005; Ladaviere *et al.*, 2007), or to form polysaccharide-drug conjugates (Mitra *et al.*, 2001; Earhart *et al.*, 2008).

2.3.1 Polysaccharides

Polysaccharides are large carbohydrate molecules constituted by repeating monosaccharide units that are linked by glycosidic bonds. Some characteristics of polysaccharides, such as having a large number of reactive groups on molecular chains, contribute to their varying chemical and biochemical composition and therefore to high diversity in their structure and properties (Liu *et al.*, 2008). Polysaccharides can be homopolysaccharides or heteropolysaccharides depending on their monosaccharide components: if the monosaccharides are all from the same type, the polysaccharide formed is called homopolysaccharide, and when the polysaccharide is composed of more than one type of monosaccharide, it is called heteropolysaccharide. The polysaccharides vary significantly in what matters to their chemical structure, source, positive or negative charge, among others, which can be observed for homopolysaccharides (Table 1) and heteropolysaccharides (Table 2).

Table 1 – Characteristics as chemical structure, source and charge of some homopolysaccharides

	Structure	Source	Charge
Chitosan	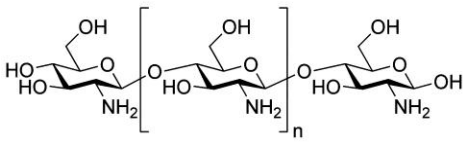	Animal	+
Dextran	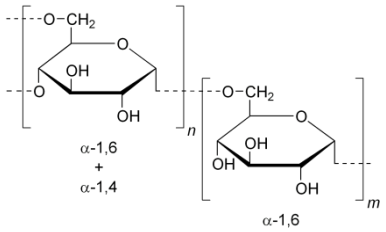	Microbial	
Pullulan	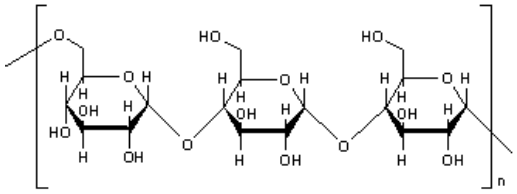	Microbial	-

Exopolysaccharides are heterogeneous and high molecular weight polymers, since they are composed of monosaccharides and some non-carbohydrate functional groups (Annarita *et al.*, 2011).

The majority of natural polysaccharides present several hydrophilic groups such as carboxyl, hydroxyl and amino groups, which endow their solubility in water and the formation of non-covalent bonds with biological tissues and mucosal membranes (Liu *et al.*, 2008). This way, the hydrophilic properties of most of the polysaccharide nanoparticles provide bioadhesion and mucoadhesion characteristics to these biomaterials, as well as giving the possibility of chemical modification of the macromolecules to bind drugs or targeting agents. The hydrophilic nanoparticles also possess the enormous advantage of extended circulation in blood, which increases the probability of passive targeting of the nanoparticles into the tumour tissues (Mitra *et al.*, 2001).

Table 2 - Characteristics as chemical structure, source and charge of some heteropolysaccharides

	Structure	Source	Charge
Hyaluronic acid	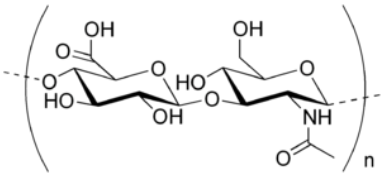	Human	-
Alginate	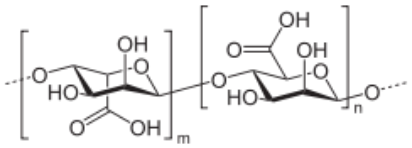	Algal	-
Gum Arabic	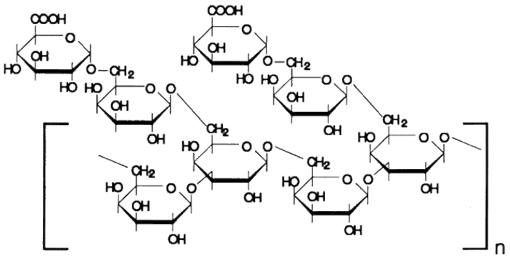	Plant	-
Xanthan gum	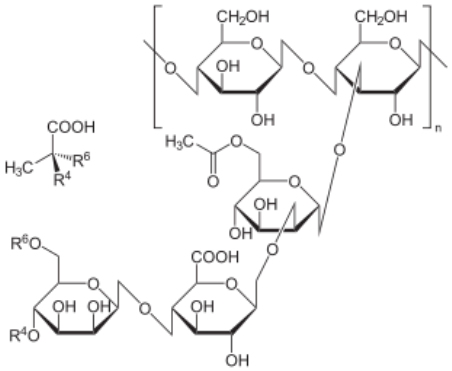	Microbial	-
Pectin	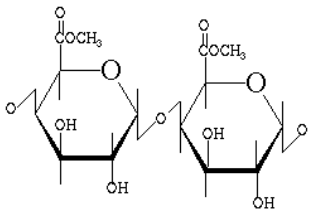	Plant	-

Besides these outstanding physical and chemical properties, polysaccharides are found in abundant sources and are low-cost processing, which convert them into good biomaterials to medical and even pharmaceutical applications (Lemarchand *et al.*, 2005; Rinaudo, 2008; Park *et al.*, 2010).

2.3.2 Chitosan nanoparticles

Chitosan has appeared as maybe the most promising biomaterial for the development of ideal hydrophilic drug vehicles for the controlled drug delivery and thus it has been highly investigated over the last two decades, approximately (Felt *et al.*, 1998; Janes *et al.*, 2001; Mitra *et al.*, 2001). Chitosan, α(1-4)2-amino 2-deoxy β-D glucan, is a deacetylated form of chitin, the second most abundant biopolymer in nature found in the exoskeleton of crustaceans and insects (Hejazi and Amiji, 2003; Bodnar *et al.*, 2005). It is a basic and functional linear polysaccharide composed of N-acetyl-D-glucosamine and D-glucosamine randomly distributed and linked units (Table 1) (Hejazi and Amiji, 2003; Park *et al.*, 2010). This polysaccharide is positively charged at neutral or basic pH, insoluble in water and organic solvents but soluble in few dilute acidic solutions (Janes *et al.*, 2001; Agnihotri *et al.*, 2004; Wilson *et al.*, 2010; Zhang *et al.*, 2010). The low solubility of chitosan at neutral and alkaline pH is because it is a weak base with a pK_a value of the D-glucosamine residue of approximately 6.2-7.0 (Hejazi and Amiji, 2003). However, in acidic medium, the amino groups are protonated, which turns chitosan into a highly charged polyelectrolyte polysaccharide (one charge for each D-glucosamine unit) (Hejazi and Amiji, 2003; Bodnar *et al.*, 2005).

Chitosan presents biological characteristics such as low or no toxicity, biocompatibility, biodegradability, low immunogenicity and antimicrobial properties (Felt *et al.*, 1998; Agnihotri *et al.*, 2004). It can be hydrolysed by lysozyme, and the degraded products of chitosan (amino sugars) are also nontoxic, nonimmunogenic and noncarcinogenic, being completely absorbed by the human body (Wilson *et al.*, 2010). Its rare positive charge converts chitosan into a special polysaccharide, since it provides strong electrostatic interaction with negatively charged mucosal surfaces and macromolecules such as DNA and RNA (Fang *et al.*, 2001; Morille *et al.*, 2008), which is an attractive feature for the treatment of solid tumours (Li *et al.*, 2009).

However, the physical and biological properties, as well as the entrapment efficiency of drugs, are greatly dependent on chitosan molecular weight, concentration, nature of the drug, degree of deacetylation (DD), among others (Hejazi and Amiji, 2003; Morille *et al.*, 2008; Park *et al.*, 2010). Chitosans with a low DD ($\leq$ 40%) are soluble till a pH value of 9.0, while the most common chitosans with higher DD ($\geq$ 85%) are only soluble up to a pH of 6.5 (Hejazi and Amiji, 2003). Normally, a low concentration of chitosan originates low encapsulation efficiency. In addition, the presence of reactive functional groups in chitosan affords great opportunity for the attachment of a hydrophobic moiety to the backbone or other chemical modifications, giving rise to a wide range of chitosan derivatives with possibly increased properties (Park *et al.*, 2010).

A large number of articles on the use of chitosan in pharmaceutical and biomedical fields and in the design of chitosan-based nanoparticle systems to incorporate anticancer drugs

as Doxorubicin, Paclitaxel and Gemcitabine have already been published (You *et al.*, 2007; Zhang *et al.*, 2007; Hu *et al.*, 2008b; Park *et al.*, 2010; Trickler *et al.*, 2010; Arias *et al.*, 2011; Arya *et al.*, 2011; Hosseinzadeh *et al.*, 2012). According to all the results obtained, it is possible to conclude that chitosan-based nanoparticles have great potential and are promising nanocarriers for antitumour drugs.

Chitosan nanoparticles for drug entrapment and delivery formulated by cross-linking in water-in-oil emulsion systems have been highly developed (Wilson *et al.*, 2010), but it has been realized that the cross-linking agents such as glutaraldehyde produce several negative effects on cell viability and decreased the stability of the entrapped macromolecules (Gan *et al.*, 2005; Hu *et al.*, 2008a). As an alternative to these limitations, ionically cross-linked nanoparticles using a negatively charged molecule such as tripolyphosphate (TPP) have been prepared by several researchers. This is a widely used procedure to prepare nanoparticles for the incorporation of biopharmaceuticals since it is immediate, simple, mild and do not include organic solvents (Alonso-Sande *et al.*, 2006; Liu *et al.*, 2008). The CS/TPP system is highly used in order to exploit the cationic properties of chitosan, as the positively charged amino groups of chitosan ionically interact with the negatively charged phosphates of TPP (Park *et al.*, 2010). Besides, TPP is non-toxic and presents quick gelling capabilities, which turns the formulation into a promising nanocarrier for the delivery of macromolecules (Gan *et al.*, 2005).

Calvo and his co-workers (Calvo *et al.*, 1997) prepared chitosan nanoparticles by ionotropic gelation by controlling the inter and intramolecular interactions created between the cationic polyelectrolyte CS and the counterion TPP. Csaba and colleagues (Csaba *et al.*, 2009) developed CS/TPP nanoparticles by ionic gelation in order to carry pDNA not only by electrostatic interactions between chitosan and DNA but also by physical entrapment upon the ionic crosslinking formed (Csaba *et al.*, 2009). Several researchers (Gan *et al.*, 2005; Hu *et al.*, 2008a; Hosseinzadeh *et al.*, 2012) prepared CS/TPP nanoparticles by ionic gelation process and studied the influence of various chitosan concentrations, chitosan to TPP ratios and medium pH on the size and morphological properties of the particles, in order to manipulate and control them to attain the highest desirable yield. Hosseinzadeh and colleagues (Hosseinzadeh *et al.*, 2012) developed chitosan nanoparticles by ionic gelation with TPP, in the presence of Pluronic F-127, for the delivery of the anticancer drug gemcitabine, having shown promising results.

2.3.3 Gum Arabic nanoparticles

Gum arabic (Gum *Acacia*) has been used for the last few years in numerous pharmaceutical formulations as an encapsulating agent, thanks to its biocompatibility, biodegradability and microencapsulating properties (Espinosa-Andrews *et al.*, 2007; Avadi *et al.*, 2010). It is a complex heteropolysaccharide (Table 2), produced by the acacia tree, with a

strongly branched structure composed of varying fractions of the simple sugars galactose, arabinose, rhamnose and glucoronic acid, as well as a covalently bound protein component (approximately 2%) (Kim and Morr, 1996; McNamee *et al.*, 1998). Gum arabic presents a high water solubility, low viscosity in aqueous solutions and good emulsifying abilities, due to the existent protein fraction (Gabas *et al.*, 2007; Kurozawa *et al.*, 2009).

Gum arabic is a weak polyelectrolyte that carries carboxylic groups, being a heterogeneous material that owns both hydrophilic and hydrophobic affinities. Some studies have shown that GA is negatively charged above pH 2.2 because the dissociation of the carboxylic groups is suppressed at lower than 2.2 pH values (Ye *et al.*, 2006). Besides, it provides retention of volatile substances and ensures effective protection of the encapsulated compound or drug against oxidation (Gabas *et al.*, 2007). However, the main problems related to the use of gum arabic in encapsulation are its high cost and limited supply.

Nanoparticles based on maltodextrin and gum arabic together are being used as catechin delivery systems (Gomes *et al.*, 2010; Peres *et al.*, 2010). In addition, the interaction between gum arabic and chitosan is starting to be exploited in a way to enhance the protein delivery (Avadi *et al.*, 2010; Avadi *et al.*, 2011; Coelho *et al.*, 2011).

The interaction between two oppositely charged polymers due to electrostatic forces is called polyelectrolyte complexation (PEC) (Liu *et al.*, 2008). When there is electrostatic attraction between two charged polysaccharides and one of them is not a strong polyelectrolyte, it may occur complex coacervation. Gum arabic is negatively charged but, even though it presents some carboxylate groups, it is not highly charged (Moschakis *et al.*, 2010). Besides, coacervation is highly influenced by the pH and ionic strength, and also by the polymer weight ratio, total concentration, flexibility and distribution, in a lower extent (Moschakis *et al.*, 2010).

2.3.4 Other polysaccharide-based NPs

Chitosan, hyaluronic acid, alginate and dextran are the most used polysaccharides for biomedical and pharmaceutical purposes, having shown superiority on most of the studies developed so far when compared to other polysaccharides. In fact, they were considered promising biomaterials in the preparation of nanovehicles for anticancer drug delivery (Chavanpatil *et al.*, 2007; Li *et al.*, 2009; Choi *et al.*, 2011). However, some other polysaccharides such as pectin, maltodextrin, heparin and guar gum have also been investigated to produce nanoparticles for biomedical purposes.

2.3.5 Hydrophobically modified polysaccharide nanoparticles

Self-assembled nanoparticles (SNPs) can be formed from amphiphilic copolymers when in aqueous environment by hydrophobic interactions between the hydrophobic fractions of them (Cho *et al.*, 2008; Liu *et al.*, 2008; Park *et al.*, 2010). These are produced by chemically attaching the hydrophobic moiety to the backbone of the hydrophilic polysaccharide (Park *et al.*, 2010), which endow the amphiphilic nanoparticles with unique characteristics such as structure and thermodynamic stability (Hyung Park *et al.*, 2006).

In the aqueous phase, nanoparticles or micelles formed exhibit their hydrophobic core domain surrounded by hydrophilic outer shells, allowing hydrophobic anticancer drugs to get entrapped inside (Kwon *et al.*, 2003; Hyung Park *et al.*, 2006). The main advantages of the SNPs composed of hydrophobically modified polysaccharides are their biocompatibility, ease of preparation and enhanced circulation time in the bloodstream, as it delays the phagocytes recognition and uptake, increasing the probability of the nanoparticles to reach the target site (Park *et al.*, 2008).

In fact, a few examples of polysaccharide-based SNPs for drug carriers such as anticancer agents have been reported to have the ability to selectively accumulate them into the tumour site throughout the EPR effect (Hwang *et al.*, 2008; Park *et al.*, 2010).

2.4 Polysaccharides as coating materials

The most common strategy for increasing the potential of nanoparticles in therapeutic applications is their surface modification (Lemarchand *et al.*, 2005; Park *et al.*, 2010). As it is known for a long time, nanoparticles should ideally present a hydrophilic surface to escape macrophage capture (Cho *et al.*, 2008), since the body recognizes hydrophobic particles as foreign and they are quickly taken up by the monocyte phagocytosis system (MPS). This way, the covalently coating of these surfaces with a hydrophilic polymer avoids or at least delays the phagocytosis process to occur (Hans and Lowman, 2002; Lemarchand *et al.*, 2005), allowing their circulation for a longer time in the body, which may increase the probability for the nanoparticles to reach their target (Kumari *et al.*, 2010).

The coating with a hydrophilic polymer such as PEG or PEG-containing copolymers is the most common strategy to reach that objective (Hans and Lowman, 2002; Kumari *et al.*, 2010). PEG is a hydrophilic nonionic polymer that presents a high biocompatibility, biodegradability and nontoxicity (Lemarchand *et al.*, 2005; Zhang *et al.*, 2010). PEGylation causes the lowering of the positive surface charge and the decrease of zeta potential, which increases the nanoparticle physical stability and biocompatibility (Janes *et al.*, 2001; Hans and

Lowman, 2002). Besides, this method also forms a hydrophilic protective layer around the nanoparticles, avoiding the absorption of proteins due to steric repulsion forces (Kumari *et al.*, 2010). However, the increase of the nanoparticles residence time in the systemic circulation is the most important factor to coat nanoparticles with PEG (Park *et al.*, 2010).

An alternative way to attain these purposes by developing carriers covered by polysaccharides has progressed in parallel to the PEG-coated nanoparticles (Lemarchand *et al.*, 2005). Polysaccharide-coated nanoparticles are especially attractive candidates for biomedical applications in general due to the biocompatibility and biodegradability they present (Ladaviere *et al.*, 2007), besides their application in drug controlled delivery. Along with their ability to reduce nanoparticle recognition by the MPS, as they are hydrophilic polymers, polysaccharide coating also ensures its stability in the blood circulation system (Ma *et al.*, 2008). Other main advantages of the nanoparticle coating with polysaccharides are steric protection, since they are able to protect the nanoparticles against non-specific interactions with proteins, and the targeting of organs and tissues in a specific way, due to their recognition and mucoadhesive properties (Lemarchand *et al.*, 2005; Ma *et al.*, 2008). Polysaccharide coatings can then be considered as a promising alternative to the PEG coatings since they endow the specific targeting (Lemarchand *et al.*, 2004; Lemarchand *et al.*, 2006), making it possible to achieve active targeting *per se*, while in pegylated nanoparticles specific ligands must be attached to the surface to enable molecular recognition and attain active targeting (Lemarchand *et al.*, 2004; Ma *et al.*, 2008). As chemical attachment of such ligands to their surface is difficult to take place because there are not reactive groups present, it turns more advantageous to use polysaccharide coatings as they present many specific receptors in certain cells or tissues (Lemarchand *et al.*, 2004). Moreover, the use of polysaccharide-coated delivery systems was proved to allow the retaining of the encapsulated drugs at the target site where they were administered (Lemarchand *et al.*, 2004).

In general, the polysaccharide is coated to the nanoparticle by dissolving in the aqueous phase where they are prepared, by nanoprecipitation or emulsion-solvent evaporation (Lemarchand *et al.*, 2004). Chitosan and its derivatives have been largely used by numerous investigators as coating agents for nanoparticles, due to their high affinity for cell membranes and positive charge, allowing the strong adsorption to the nanoparticles (Janes *et al.*, 2001). Dextran and heparin were also already utilized to coat the surface of several nanoparticles for biomedical applications, such as cancer treatment (Lemarchand *et al.*, 2005), having been proved to, in fact, induce a decrease of protein adsorption and promote the enhancement of the blood residence time of the nanocarriers (Lemarchand *et al.*, 2004; Lemarchand *et al.*, 2006).

In addition to the increasing new methods for cancer diagnosis and treatment, the advanced technologies for tumour imaging and early detection are also being explored. The coating of nanoparticles with some special functionalities can be a possible solution to attain

these purposes. The molecular imaging can be improved by the use of nanomaterials or coatings of the nanomaterials and is significantly changing the major paradigm of Medicine from the treatment of what is seen in the moment to the previous detection and prevention (Barreto *et al.*, 2011).

2.5 Polysaccharide-drug conjugates

In the sequence of the new promising anticancer drug carriers, such as polysaccharide nanoparticles, the conjugation of the drugs to polymer carriers has also been highly studied (Sinha *et al.*, 2006). The water solubility of hydrophobic drugs that are nowadays in use, such as doxorubicin and paclitaxel, can be improved by their conjugation to hydrophilic carriers, resulting in an enhanced efficacy of the administered drug (Duncan, 2006). Besides, it is expectable that, directly conjugating the anticancer drug to polymers such as polysaccharides as targeting ligands, an improvement on the drug targeting to the tumour occurs, the toxicity is reduced and the mechanisms of drug resistance can be overcome (Duncan, 2006; Sinha *et al.*, 2006). In addition, it was already proved that conjugates can circulate in blood much longer than free drugs, which can result in a significantly higher concentration of drug in tumours. However, the most important advantage of polymer-drug conjugates is the fact that they also present the ability of passively accumulate at the tumours due to the EPR effect (Park *et al.*, 2010).

Thanks to these advantageous characteristics, several polymer-drug conjugates have already entered into phase I/II clinical trials, being a special potential attributed to these conjugates. However, most studies that have been carried in the early stage failed to show their enhanced ability of anticancer drug delivery and this attachment of a ligand to the polymeric drugs has not been very effective in animal studies (Park *et al.*, 2010). This may be due to a decrease in the biological activity of drugs, to the chemical structure changes or even to the inactivation of the cell-binding domains caused by the conjugation process of the targeting moiety (Sinha *et al.*, 2006; Park *et al.*, 2010). This way, the drugs should be conjugated to the polymers in a way that do not affect the receptor/ligand recognition site, letting them accumulate at the tumour site through the EPR, or even to produce ternary nanocarriers composed of the polymer, the active chemotherapeutic drug and a targeting moiety (Sinha *et al.*, 2006). Compared to the ligand-drug conjugates, this ternary system is more attractive since the drugs are physically entrapped, preserving their activity; the targeting moieties can be perfectly adjusted on the surface, allowing the binding to the target cells; many drugs can be loaded into the hydrophobic core of the particle, increasing the water solubility; they maintain their small

size, which turns the passive targeting through tumour tissues possible to occur but not through normal vasculature (Park *et al.*, 2010).

The main problem of the conjugation between drugs and polymers, that is slowing down further development, is related with the toxicity and/or the immune response that the polymers, unlike PEG, can cause (Duncan, 2006). Besides, it can occur a problem on the drug loading or in the use of an inappropriate polymer-drug linker, since if it is too stable, the drug liberation does not occur when the conjugate is targeted, and if it is quickly degraded in aqueous solutions it can lead to premature drug release (Duncan, 2006). For these reasons, the decision and the careful design of the structures to be used must be taken prudently, studying, validating their chemical characterization and assuring their safety before proceeding into clinical trials (Duncan, 2006).

2.5.1 Chitosan-drug conjugates

As chitosan presents all the unique physicochemical and biological properties already referred, its conjugation with anticancer drugs such as doxorubicin and gemcitabine has also been an important focus of attention (Park *et al.*, 2010). In fact, chitosan-drug conjugates have been recently developed and extensively investigated (Son *et al.*, 2003). These allowed the physical entrapment of the anticancer drug into the self-assembled nanoparticles, being then accumulated in the specific tumour tissue thanks to the EPR effect (Son *et al.*, 2003). Lee and work partners (Lee *et al.*, 2008) developed a new system for the oral delivery of paclitaxel (PTX) by chemically conjugating it with low molecular weight chitosan (LMWC). Arya and co-workers (Arya *et al.*, 2011) produced chitosan nanoparticles using an ionic gelation method to encapsulate gemcitabine and conjugated HER2, an epidermal growth factor receptor, having the conjugated nanoparticles presented a better selectivity in comparison to the unloaded (Arya *et al.*, 2011). Arias et al. (Arias *et al.*, 2011) prepared chitosan nanoparticles by coacervation with sodium sulphate in order to entrap gemcitabine, having reached reasonable entrapment efficiency values.

2.6 Gemcitabine

Gemcitabine (2',2'-difluoro-2'-deoxycytidine) is a nucleoside metabolic inhibitor that demonstrated to have antitumour activity (Eli Lilly, 2011). It is marketed as Gemzar® (gemcitabine for injection) by Eli Lilly and Company (Indiana, USA) for the treatment of

several solid tumours including ovarian, breast, non-small cell lung, pancreatic cancers, among others.

The empirical formula of gemcitabine HCl (Gemzar®) is $C_9H_{11}F_2N_3O_4 \cdot HCl$, the molecular weight is 299.66 $g.mol^{-1}$ and its structural formula is the one presented in Figure 3.

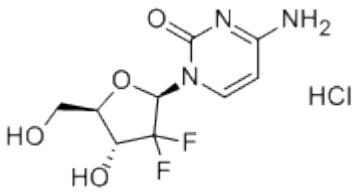

Figure 3 – Chemical structure of gemcitabine HCl (SelleckChem, 2012).

It is soluble in water, slightly soluble in methanol and almost insoluble in ethanol and polar organic solvents, since it is hydrophilic.

Gemcitabine is used in combination with carboplatin for ovarian cancer, paclitaxel for the treatment of breast cancer, cisplatin for small-cell lung and as a single-agent for pancreatic cancer (Eli Lilly, 2011) and presents a dual mechanism of action, which turns it into a potent chemotherapeutic agent (Trickler *et al.*, 2010). For the pancreatic cancer therapy, Gemzar is indicated as first-line treatment (Burris *et al.*, 1997) for patients with locally advanced or metastatic adenocarcinoma of the pancreas, being also used in patients previously treated with 5-FU. It should be administered at a dose of 1000 mg/m^2 over 30 minutes once weekly for up to 7 weeks, followed by a week of rest from the treatment and subsequent cycles once weekly for 3 in 4 weeks (Eli Lilly, 2011).

However, the major drawbacks to the use of gemcitabine in clinical treatment are related to its rapid metabolism, short half-time and low permeability, which leads to a high dose of administered drug need, resulting in unwanted side-effects (Trickler *et al.*, 2010; Sloat *et al.*, 2011). Besides, since gemcitabine is a highly hydrophilic molecule with a pKa of 3.6 and a low molecular weight, it requires nucleoside transporters in the membrane to reach the cells (Pastor-Anglada *et al.*, 2004; Reddy *et al.*, 2007; Hosseinzadeh *et al.*, 2012). Moreover, this is the most common factor for the development of gemcitabine resistance (Mackey *et al.*, 1998). For these reasons, it became imperative to synthesize gemcitabine derivatives to chemically protect its 4-amino group from metabolic inactivation (Stella *et al.*, 2007), which have been proved to present a higher cytotoxic activity but a decrease in the water solubility. This way, the development of new approaches such as nanoparticles for the delivery of gemcitabine to specific tumour cells has been recently carried (Gang *et al.*, 2007; Reddy *et al.*, 2007; Stella *et al.*, 2007; Arias *et al.*, 2008; Wang *et al.*, 2009; Arias *et al.*, 2011; Sloat *et al.*, 2011; Hosseinzadeh *et al.*, 2012). However, no alternative and efficacious formulation other than Gemzar® is available on the market yet.

3 Materials and Methods

3.1 Materials

Medium molecular weight chitosan (MMWC) (248 kDa, DD 93%, apparent viscosity 150 cps) and low molecular weight chitosan (LMWC) (20 kDa, DD 92%, viscosity 78 cps) were both purchased from Altakitin (Portugal). Gemcitabine hydrochloride (Gemzar®) S1149 (MW 299.7, purity ≥ 99%) was purchased from Selleck Chemicals LLC. Gum arabic 51201 (MW ≈ 250 kDa), sodium tripolyphosphate (TPP) (MW 367.86, tech., 85%), polysorbate 80, glacial acetic acid > 99.7% (MW 60.05), sodium hydroxide, sodium chloride and phosphate buffered saline (PBS) were purchased from Sigma-Aldrich (Germany).

All aqueous solutions were prepared in deionized and filtered ultrapure Milli-Q water (Milli-Q Academic, Millipore, France).

3.2 Preparation of Nanoparticles

The suitable masses of chitosan of both molecular weights 20 and 248 kDa were dissolved in 1% (v/v) acetic acid aqueous solution to attain the desired final concentrations and the pH of the chitosan solutions adjusted to 4.5-5 with 10% sodium hydroxide aqueous solution. TPP and GA solutions were prepared in ultrapure Milli-Q water.

The preparation of the nanoparticles for characterization was performed by dropwise addition of TPP or GA into the chitosan solutions, volume proportion of 1:2.5 CS/TPP (final volume of 3.5 mL) and 1:1 CS/GA nanoparticles (final volume of 5.0 mL), followed by magnetic stirring at 250 rpm for 15 min at room temperature. The CS/polymer mass concentration ratios tested were of 4, 10, 20, 50 and 100 for the CS248/TPP nanoparticles, with a CS concentration of 1 $mg.mL^{-1}$ and of 4, 10, 20 and 5, 12.5 and 25 for the CS20/TPP NPs with

CS concentrations of 1 and 1.25 $mg.mL^{-1}$, respectively. For the CS/GA system, the tested ratios were 0.75, 1 and 1.5 for the both CS concentrations of 0.3 and 0.6 $mg.mL^{-1}$.

For the gemcitabine-loaded nanoparticles, the entrapment procedure was followed by adding the gemcitabine to the TPP or GA solution, depending on the case, and following the same procedure as for the unloaded nanoparticles preparation. The chosen ratios were of 20 for CS/TPP, i.e. CS 0.1% (w/v) and TPP 0.005% (w/v) and of 0.75 with a CS concentration of 0.3 $mg.mL^{-1}$ for the CS/GA system, it means, CS 0.03% (w/v) and GA 0.04% (w/v). The magnetic stirring was maintained at 250 rpm but the reaction time increased to 1 hour. The gemcitabine was added from a stock solution to have a 0.01% (w/v) final concentration on the solutions, i.e. 0.1 $mg.mL^{-1}$ or 333.71 μM. The presence of gemcitabine in the final solutions was of 8.7% (w/w) and 12.5% (w/w) in the CS/TPP and CS/GA system, respectively.

The coating of the particles' surface with polysorbate 80 was carried out by adding it in the end of the 1 hour reaction, testing two different concentrations of polysorbate 80: 0.2 and 1% (v/v).

The preparation of the nanoparticles was run under a laminar flow chamber and all experiments were performed in triplicate.

3.3 Physicochemical characterization

The size, polydispersity index, zeta potential and morphological appearance were the parameters used to characterize the produced nanoparticles.

3.3.1 Particle size

Dynamic light scattering (DLS) is a well established technique to determine molecules and particles size (hydrodynamic diameter) and size distribution of nanoparticles in dispersion or solution (Malvern, 2012). It is based on the fact that the particles in solution under Brownian motion, when striked with a light, undergo interactions and cause deflections in the light original direction. This change of the wavelength is measured by the intensity of the scattered light in that microsecond time range and depends on the size of the particles. For spherical monodisperse particles, the hydrodynamic diameter, d_p, can be determined from the diffusion coefficient, D, which is characteristic of the Brownian motion, by the Stokes-Einstein relation (Equation 1).

$$D = \frac{k_B T}{3\pi\eta d_p} \quad (1)$$

where k_B is the Boltzmann constant, T the absolute temperature and η the viscosity.

In this work, the size and polydispersity index were measured by a ZetaSizer Nano ZS (Malvern Instruments, Worcestershire, UK), using a clear disposable zeta cell at approximately 25 °C and an angle of the laser incidence of 173°. Mean values for each preparation were obtained by at least duplicate measurements of three different batches.

3.3.2 Zeta potential

Particles dispersed in an aqueous solution acquire a surface charge, which is a result of the ionization of surface groups or adsorption of charged species. This way, each particle presents an electrical layer, constituted by an inner and an outer region, the stern and the diffuse layer, respectively. The zeta potential is the electric potential at the hypothetical boundary that exists between the particle with its ion atmosphere and the bulk solution (Mu and Feng, 2001).

Electrophoretic mobility is one of the methods that are normally used to determine the zeta potential of the particles, in order to characterize their surface properties and stability in suspensions. An electrophoresis experiment is run by applying an electric field across the sample, taking into account the resulting motion and electrical phenomena of each material. The velocity of the charged particles that are suspended in the electrolyte and migrate towards the opposite charge electrode is measured by Laser Doppler Velocimetry. However, forces such as viscosity tend to oppose this movement, and when the equilibrium between them is attained, the particles move at a constant velocity, which is named electrophoretic mobility (U_E). The zeta potential can then be calculated by the Henry equation (Equation 2).

$$U_E = \frac{2\varepsilon\xi f(ka)}{3\eta} \tag{2}$$

where ε is the dielectric constant, ζ the zeta potential, η the viscosity and f(ka) the Henry's function, which for aqueous medium and moderate electrolyte concentration is considered 1.5. In that case, the zeta potential can be determined from the electrophoretic mobility measured by the Smoluchowski equation (Equation 3).

$$\xi = \frac{\eta U_E}{\varepsilon} \tag{3}$$

Zeta potential magnitude indicates the potential stability of the analysed system, being a suspension considered stable if it presents a zeta potential higher than 30 mV in modulus. If this value is between -30 and 30 mV, the system is considered unstable because when it is weakly charged there is no force to prevent the particles to aggregate.

The zeta potential was also measured using a ZetaSizer Nano ZS (Malvern Instruments, Worcestershire, UK), making use of Laser Doppler Velocimetry. All the determinations were performed in a clear disposable zeta cell at approximately 25 °C and a light scattered at an angle of 17°. Mean values for each preparation were also obtained by at least duplicate measurements of three different batches.

3.3.3 Morphologic analysis

Transmission Electron Microscopy (TEM) is a microscopy technique that produces a real space image of the entire object, including the surface and the internal structures, allowing the characterization of the total structure geometry. It is based on the interaction of an incoming electron beam with the sample through which it passes, being the intensity influenced by its thickness and by the concentration of atoms in that sample. Since the beam crosses the entire sample thickness and the electrons interact with single atoms, it needs to be thin or it will absorb too much of the electron beam. The electrons come from a single source (the emission source, that is the illumination system) and they travel in a vacuum system, so all the waves in the incident beam are in phase with each other. The difference in the emitted waves from different specimens is due to elastic or nonelastic scattering processes, and their study gives important information about the crystal structure and defects, as well as the chemical composition of the surface, respectively (Cahn and Haansen, 1996). The samples are typically put on support grids made of Cu, that possess an ultramicrotomy mesh. Samples of biological origin are generally negatively stained by uranyl acetate or phosphotungstic acid.

In this work, a sample of 10 µL of each prepared solution was placed over a carbon coated copper TEM grid (Formvar/Carbon on 400 mesh Cu (50) from Agar Scientific), and stained with a 2% (v/v) phosphotungstic acid solution. The images were observed on a TEM Yeol Yem 1400 (80 kV) (Tokyo, Japan) with a Digital Camera Orious 1100 (Japan).

3.4 Gemcitabine-loading efficiency

Each suspension was centrifuged at 14,000 rpm for 30 minutes using a MiniSpin Plus (Eppendorf) centrifuge to remove the extra TPP or GA and unencapsulated gemcitabine. The absorbance of the supernatant was measured to indirectly calculate the encapsulation efficiency for all the preparations, also taking into account the almost insignificant quantity of escaped drug after the washing of the pellets with ultrapure water.

UV-vis spectra of gemcitabine in the range of 200-400 nm was analysed by using a UV-1700 PharmaSpec UV-Vis spectrophotometer from Shimadzu (Japan), using HOQ 310H quartz

cells (Hellma) of 1 cm path length. The concentration of gemcitabine in solution was determined by the peak area from the absorbance UV-Vis signal correlated with the calibration curve of gemcitabine in water (Appendix A - Figure 14) that was prepared under identical conditions between 5 and 100 µg/mL.

The gemcitabine encapsulation efficiency (%) is calculated by the Equation 4.

$$\text{Encapsulation efficiency (\%)} = \frac{\text{Encapsulated drug (mg)}}{\text{Total drug in solution (mg)}} \times 100 \quad (4)$$

3.5 Process yield determination

The calculation of the process yield was run following a procedure adapted from Alonso-Sande and co-workers (Alonso-Sande *et al.*, 2006), centrifugating the entire nanoparticles suspension (15,000 g, 25 °C, 1 h) of the gemcitabine-loaded particles and gemcitabine-loaded particles with polysorbate 80 coating. A Thermo Scientific Heraeus Multifuge X1R centrifuge was used. Consequently, the supernatant was discarded and the sediments freeze dried for 24 h, after being freezed overnight at -80 °C, obtaining the difference of the theoretical solids weight and the actual nanoparticles weight. The final mass of the nanoparticles was measured and it turned possible to calculate the process yield and the loading capacity by Equation 5 and Equation 6, respectively.

$$\text{Process yield (\%)} = \frac{\text{Nanoparticles weight (mg)}}{\text{Total solids weight (mg)}} \times 100 \quad (5)$$

$$\text{Drug loading capacity (\%)} = \frac{\text{Encapsulated drug (mg)}}{\text{Total nanopartices weight (mg)}} \times 100 \quad (6)$$

3.6 Gemcitabine release from the particles

Drug release experiments of the chitosan nanoparticles were run using a dialysis bag, the Float-A-Lyzer of 2 mL and a 100 kDa molecular weight cut off (MWCO) with Biotech Grade Cellulose Ester (CE) Membranes from Spectrum Labs. The membranes were washed in ultrapure water for 12 hours before being used and with Phosphate Buffered Saline (PBS) 1 hour before the beginning of the experiment run with PBS as the receiving phase. 2 mL of the nanoparticles aqueous suspension were added into the membrane and the outside space was filled with 6 mL of water or PBS at pH 7.4, in a way to mimic the physiological medium where the particles are being released when administered. It was continuously stirred at 200 rpm at

room temperature or 37 °C, depending if the receiving phase was water or PBS, respectively. 1 mL samples were taken from the outside medium at different time intervals (0, 0.25, 0.5, 0.75, 1, 1.5, 2, 4, 6, 8, 10, 24, 30, 48 and 58 h, when needed) to obtain the UV-Vis spectra in the range of 200-400 nm, using the same spectrophotometer, and returned. This way, it turned possible to determine the gemcitabine concentration that had passed the membrane at each time by correlating the peak area from the absorbance signal and the gemcitabine calibration curve in water or PBS, depending on each case (Appendix A - Figure 14 and Figure 15, respectively). The gemcitabine released percentage at each time is then calculated from the Equation 7.

$$\text{Gemcitabine released at time t (\%)} = \frac{|\text{Gem}|_t}{|\text{Gem}|_f} \times 100 \quad (7)$$

where $|\text{Gem}|_f$ is the gemcitabine final concentration if all the present drug is released.

As controls, drug-free particles and the gemcitabine alone were used.

3.7 Cytotoxicity studies

Adherent cell cultures of a human pancreatic cell line (S2013) were maintained in DMEM with 10% heat-inactivated fetal bovine serum (FBS) at 37 °C in a humidified 5% CO_2 incubator. No antibiotics were used in growing and maintaining the cell cultures. Experiments were run in 96-well assay plates, where exponentially growing cells were seeded for an incubation period of 24 h at a density of $1x10^4$ cells/mL before treatment with free gemcitabine, bare CS/GA or CS/GA-p80, and gemcitabine-loaded CS/GA and CS/GA+p80 nanoparticles. The samples of nanoparticles and free gemcitabine were diluted in DMEM at final concentrations ranging from 5 nM to 10 μM and the cells were incubated with these samples for 48 h. Not exposed cells were also included in all assays as no-treatment controls and all samples were tested in triplicates. Cytotoxic effect following incubations was assayed using PrestoBlue™ (PB) cell viability reagent (Invitrogen, USA) and protein-binding dye sulforhodamine B (SRB). The PB reagent becomes highly fluorescent when modified by the reducing environment of the viable cells, and that change was measured by fluorescence (560/590 nm), while the methodology using SRB was based on the staining cellular protein, which gives an indirect estimation of the cell number and degree of cytotoxicity. Following the exposure period, adherent cells were fixed, washed and stained with SRB. The incorporated dye was then solubilized and the absorbance measured at 560 nm. Concentration-response curves using non-linear regression analysis were obtained and the concentration inhibiting cell survival by 50% (IC_{50}), together with the concentration inhibiting the net cell growth by 50% (GI_{50}) were

determined. IC_{50} and GI_{50} are the concentrations of test drug where Equations 8 and 9, respectively, are applicable.

$$\frac{T}{C} \times 100 = 50\% \quad (8)$$

$$\frac{(T-T_0)}{(C-T_0)} \times 100 = 50\% \quad (9)$$

where T is the quantitative measurement at the end of the incubation period, T_0 is the quantitative measurement at the time of test drug addition and C is the quantitative measurement in the control wells.

3.8 Statistical analysis

Statistical analysis was performed by using one-way analysis of variance (ANOVA) or two-tailed Student's t-test, and by Tukey's multiple comparison tests, when applicable, considering a confidence interval of 95% (SPSS Statistics 17.0, SPSS Inc., Chicago, IL). P values of less than 0.05 and 0.001 were considered significant and very significant, respectively.

4 CS/TPP system

4.1 Unloaded CS/TPP nanoparticles

A detailed study was developed in order to identify the adequate conditions to control and manipulate the physicochemical characteristics of the chitosan/tripolyphosphate (CS/TPP) nanoparticles. Therefore, the influence of several parameters such as CS molecular weight, CS concentration and CS/TPP mass concentration ratio on the nanoparticles' physicochemical properties have been analysed.

The formation of CS/TPP NPs occurred spontaneously upon the dropwise addition of this crosslinking agent into the chitosan solution. A change on the solution from clear to opalescent was noticed, which indicates a physical state alteration of the chitosan when the negative TPP ions are added by an ionic gelation method, forming nanoparticles.

4.1.1 Size and zeta potential characterization

For the characterization of these particles, several TPP concentrations were tested for the different concentrations of chitosan and both for the chitosan of 248 and 20 kDa. The attained results of size, polydispersity index and zeta potential for all the formulations using the MMWC are shown in Table 3.

Table 3 – Physicochemical characterization of CS248/TPP nanoparticles. Data represented as mean ± SD (n=3)

Ratio CS/TPP	|CS| ($mg.mL^{-1}$)	|TPP| ($mg.mL^{-1}$)	Mean diameter (nm)	Polydispersity index	Zeta potential (mV)
4	1	0.25	490 ± 5	0.7 ± 0.5	50 ± 1
10	1	0.1	434 ± 6	0.7 ± 0.4	63 ± 1
20	1	0.05	288 ± 5	0.6 ± 0.3	59 ± 2
50	1	0.02	515 ± 18	0.7 ± 0.5	43 ± 2
100	1	0.01	442 ± 12	0.7 ± 0.4	49 ± 2

The mean diameters of the nanoparticles formed were in the range of 288-515 nm and the zeta potential values were in the range of 43-63 mV for the different formulations, which reflect the NPs stability. The inexistence of a linear tendency on the mean diameter and zeta potential in function of the increasing CS/TPP ratio, or decreasing TPP concentration, for the same concentration of chitosan (1 $mg.mL^{-1}$) can be observed. An increase in the mean diameter of the formed particles was expected for increasing TPP concentrations, since the higher amount of anionic phosphate groups of TPP cause more interaction with the positive amino groups of chitosan, leading to a reduction of the zeta potential and a favoured attraction between molecules. This increase tendency was just observed for a TPP concentration in the range between 0.05 and 0.25, although the results are not significantly different ($P > 0.05$) for the various ratios. In fact, some other studies on the modulation and control of particle size, surface charge and morphologic properties of CS/TPP nanoparticles have used a higher TPP concentration as the minimum one tested.

Hosseinzadeh and colleagues (Hosseinzadeh *et al.*, 2012) tested the effect of TPP concentration on chitosan (at 1 $mg.mL^{-1}$) nanoparticles in the range of 0.15-0.30 $mg.mL^{-1}$, reporting an increasing size and decreasing zeta potential as increasing the TPP concentration. Besides, Calvo and his co-workers (Calvo *et al.*, 1997) have shown that, for this same concentration of chitosan, TPP concentrations higher than 0.5 $mg.mL^{-1}$ produced aggregated solutions. Based on that reported values, the higher TPP concentration tested in this study was of 0.25 $mg.mL^{-1}$, being possible to predict aggregation phenomena for higher concentrations than that, due to the increase in the particles size and polydispersity index.

Based on these facts, the CS/TPP ratio of 20 was considered the most adequate for the formation of nanoparticles, since it presented the lowest mean diameter value of the tested formulations, being the selected one to the following gemcitabine-loading experiments for the MMWC.

For the LMWC (CS20), the narrower range of TPP concentration between 0.05 and 0.25 was tested, for both chitosan concentrations of 1 and 1.25 mg.mL^{-1} (Table 4).

Table 4 – Physicochemical characterization of CS20/TPP nanoparticles. Data represented as mean ± SD (n=3)

Ratio CS/TPP	|CS| (mg.mL^{-1})	|TPP| (mg.mL^{-1})	Mean diameter (nm)	PdI	ZP (mV)
4	1	0.25	214 ± 3	0.5 ± 0.2	52 ± 1
10	1	0.1	324 ± 6	0.5 ± 0.3	58 ± 1
20	1	0.05	443 ± 9	0.6 ± 0.3	56 ± 2
5	1.25	0.25	243 ± 3	0.5 ± 0.3	54 ± 1
12.5	1.25	0.1	281 ± 5	0.5 ± 0.3	58 ± 2
25	1.25	0.05	515 ± 8	0.6 ± 0.3	59 ± 2

Table 4 shows that the general tendency of the CS/TPP nanoparticles is to increase their size when increasing the CS/TPP ratio (decreasing the TPP concentration) for both CS concentrations of 1 and 1.25 mg.mL^{-1}. This mean diameter growth was not statistically significant for CS 1 mg.mL^{-1} ($P > 0.05$) but it was for CS 1.25 mg.mL^{-1} ($P < 0.05$). This tendency is the opposite of the one observed for MMWC nanoparticles, which can possibly be explained by the fact that a lower molecular mass chitosan molecule (for the same DD ≈ 93%) presents less available cationic amine groups to be neutralized (Hu *et al.*, 2008a) and, thus, requires a lower concentration of TPP to reach the same neutralization degree. Moreover, several authours (Calvo *et al.*, 1997; Xu and Du, 2003; Wu *et al.*, 2005; Hu *et al.*, 2008a) have reported that the formation of nanoparticles is only possible within some moderate concentrations of CS and TPP and a higher quantity of TPP added may result in a stronger interaction, producing smaller NPs. Besides, the chitosan concentration may present a higher influence on this size increase when the LMWC is utilized, as it was stated by Gan and co-workers (Gan *et al.*, 2005). In fact, for the NPs with a higher chitosan concentration (1.25 mg.mL^{-1}), the mean diameter was generally higher, when compared to the 1 mg.mL^{-1} concentration, although it is not a significant difference ($P > 0.05$).

The same increase tendency occurs when regarding the zeta potential values for both chitosan concentrations (Table 4). Between the CS 1 and 1.25 mg.mL^{-1}, the nanoparticles with higher CS concentration also presented a general higher zeta potential value, although they are not significantly different ($P > 0.05$). This is in conformity with the expected, since at the same degree of deacetylation, the higher the CS concentration is, the more -NH_3^+ groups are on CS molecules to be neutralized, which leads to a higher need of TPP polyanionic phosphate groups.

This way, a lower degree of neutralization of the existent $-NH_3^+$ groups occurs, leading to a higher positive charge at the surface of the nanoparticles (increased zeta potential).

These findings corroborate the reported results made by Hu and his co-workers (Hu *et al.*, 2008a) and Hosseinzadeh et al. (Hosseinzadeh *et al.*, 2012), that have shown a linear increase of the particle size and zeta potential when increasing the CS concentration. However, Gan and his colleagues (Gan *et al.*, 2005) reported a zeta potential of CS/TPP nanoparticles decrease and a linear increase of size with increasing CS concentration and CS/TPP weight ratio, which may be due to some differences in molecular weights and deacetylation degrees of the CS used. In fact, Gan and his co-workers (Gan *et al.*, 2005) developed an extensive characterization for the manipulation of CS/TPP NPs characteristics using different CS/TPP ratios and different CS concentrations for low, medium and high molecular weight chitosans. They reported a higher size for the HMWC, followed by the medium and only then the LMWC, which confirms the general decrease in the mean diameters of the CS/TPP NPs obtained when using MMWC and LMWC.

The selected CS/TPP ratio from the studied formulations to the consequent work was the 4/1 for the chitosan of 20 kDa, since it presented the most favourable size for the encapsulation and delivery of a drug.

4.1.2 Morphologic analysis

The TEM micrographs for the morphologic examination of the unloaded CS/TPP using both molecular weight chitosan nanoparticles at the CS/TPP concentration ratio of 20 and 4, respectively, are shown in Figure 4.

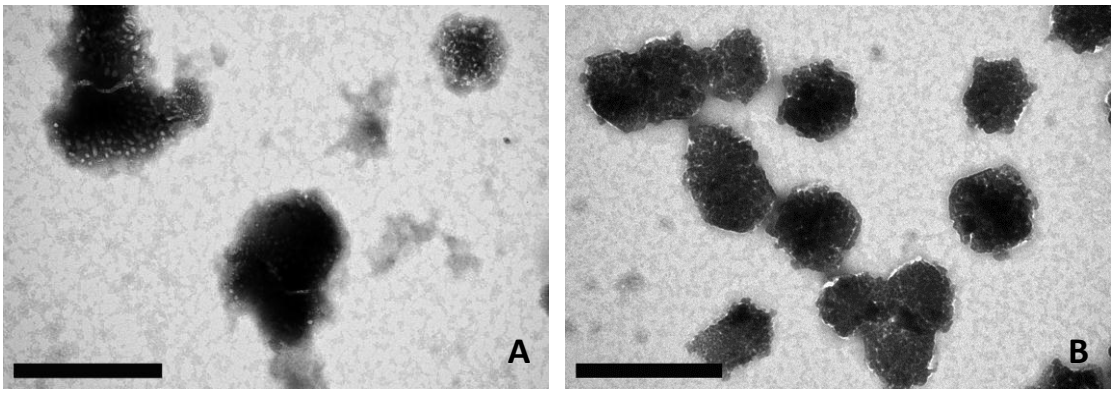

Figure 4 – TEM micrograph of free (A) CS248/TPP and (B) CS20/TPP nanoparticles (The scale bar corresponds to 400 nm).

The morphologic analysis of these CS/TPP NPs revealed an imperfect spherical shape with a degree of polydispersity. It is possible to observe an aggregate of two and three single particles, which can present an evidence of the formation of polyhydrons, instead of perfect spheres. This happening was already reported by Gan and his co-workers (Gan *et al.*, 2005), and

can be due to a semi-crystal formation and growth in consequence of the nucleation through ionic gelation.

4.2 Gemcitabine-loaded CS/TPP nanoparticles

4.2.1 Size and zeta potential characterization

The size, polydispersity index and zeta potential values for the gemcitabine-entrapped CS/TPP nanoparticles are presented in Table 5. It is shown for both MMWC and LMWC.

Table 5 – Physicochemical characterization of gemcitabine-loaded CS/TPP nanoparticles. Data represented as mean ± SD (n=3)

CS molecular weight (kDa)	Mean diameter (nm)	PdI	Zeta potential (mV)
248	373 ± 4	0.6 ± 0.5	43 ± 1
20	594 ± 5	0.4 ± 0.2	42 ± 1

From comparing the obtained values of Table 3, Table 4 and Table 5, it can be concluded that the size distribution of the CS/TPP nanoparticles were not significantly different ($P > 0.05$) with the presence of gemcitabine. However, the mean diameter increased and the zeta potential decreased. This statistically significant decrease ($P < 0.05$) in zeta potential values when gemcitabine was added can be explained by its adsorption to the NPs surface.

The CS/TPP-Gem nanoparticles using LMWC have shown much higher diameters when compared with the unloaded CS/TPP NPs. These are inconstant results, which can be due to the lower molecular mass and viscosity of the molecule. Hu and partners (Hu *et al.*, 2008a) reported no noticeable difference among the particle sizes when CS molecular weights of 50, 100 and 150 kDa were used but significant difference was observed between the CS molecular mass of 30 and 50 kDa and between 150 and 300 kDa. They attributed this fact to the shearing degradation of chitosan during the magnetic stirring of the CS and TPP mixture, presuming that the polymer has to be long enough to resist the shear stress it is exposed to. For these reasons, it can be concluded that chitosans with molecular weights lower than 30 kDa, as in this case, may not be long enough and, thus, not appropriate in the formation of CS/TPP nanoparticles. These cumulative facts led to the choice of discarding the LMWC and picking the 248 kDa CS for the following studies (CS248 is now referred to as just CS).

Arias and his work partners (Arias *et al.*, 2011) reported, by the determination of its free energy of interaction, that chitosan in NPs prepared by coacervation is mainly considered hydrophobic, favouring the attraction of the nanoparticles to each other, when not considering electrostatic forces. On the other hand, the anticancer drug gemcitabine can be positively charged, by the protonation of its $–NH_2$ group, which results in a not favourable electrostatic interaction between the hydrophilic gemcitabine and the hydrophobic nanoparticle surface of CS NPs, which confirms its poor adsorption onto the nanoparticles. For this reason, the coating of the nanoparticles' surface with the nonionic tensioactive polysorbate 80 was studied at 1% (v/v). The physicochemical characterization of both uncoated and p80-coated NPs is presented in Table 6.

Table 6 – Physicochemical characterization values for CS/TPP-Gem NPs uncoated and coated by polysorbate 80 at 1% (v/v). Data represented as mean ± SD (n=3)

p80 concentration (% v/v)	Mean diameter (nm)	PdI	ZP (mV)
0	373 ± 4	0.6 ± 0.5	43 ± 1
1	224 ± 2	0.7 ± 0.6	40 ± 1

It can be observed that the size distribution and ZP values of the CS/TPP nanoparticles were not significantly altered ($P > 0.05$) by adding p80, although the mean diameter significantly decreased ($P < 0.05$). This fact can possibly be explained by the formation of a gel, leading to lesser water uptake, which causes smaller swelling, as stated Hosseinzadeh and co-workers (Hosseinzadeh *et al.*, 2012).

The encapsulation efficiency, loading and process yield were not calculated due to the impossibility to separate effectively CS/TPP nanoparticles from the aqueous suspension, since a sediment was not obtained in the tested centrifugation conditions.

4.2.2 Morphologic analysis

The TEM micrographs for the morphologic examination of the gemcitabine-loaded CS/TPP nanoparticles with and without p80 are shown in Figure 5.

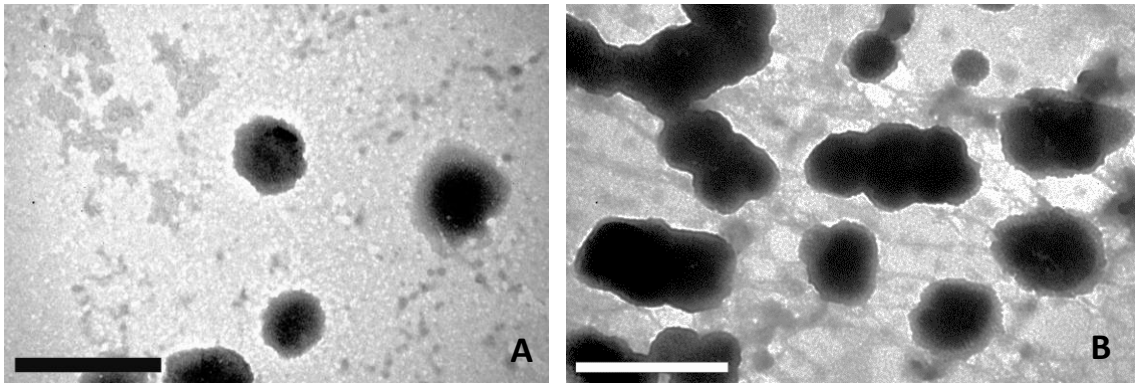

Figure 5 – TEM micrographs of gemcitabine-loaded (A) CS/TPP nanoparticles and (B) CS/TPP-p80 nanoparticles (The scale bar corresponds to 400 nm).

These TEM images revealed spherical and uniform CS/TPP nanoparticles with a reduced polydispersitivity. Besides, the CS/TPP-Gem particles have changed their properties upon the final addition of polysorbate 80, which may have resulted in their partial aggregation, suspicion based on their increased polydispersity index and on the comparison between the TEM micrographs of both uncoated and coated nanoparticles.

The mild and immediate ionic gelation procedure used to produce CS/TPP nanoparticles has shown several advantages, such as the ease of control and manipulation of their sizes and physicochemical properties to produce the highest yield nanoparticles. However, the impossibility to isolate the nanoparticles from the aqueous suspension by centrifugation, not being possible to calculate the entrapment efficiency, process yield and drug loading, presented strong disadvantages to the development of gemcitabine nanocarriers by this methodology. In addition, the indication of a semi-crystallisation mechanism during the particle formation and growth can have several negative implications on the drug encapsulation and *in vitro* release studies, as it was already reported by Gan and his co-workers (Gan *et al.*, 2005). Besides, Chen and colleagues (Chen *et al.*, 2007) stated that CS/TPP nanoparticles present low stability and mechanical strength, which can limit the drug delivery.

Thus, further studies were proceeded with the CS/GA system, a new type of chitosan nanoparticles using gum arabic as an opposite charged anionic polymer for complex coacervation, instead of ionic gelation method by an electrolyte such as TPP. GA has the advantage of presenting more interaction sites and negative charge for the interaction with chitosan (Avadi *et al.*, 2010), which can turn CS/GA nanosystem a promising alternative when compared to the extensively investigated CS/TPP nanoparticles for the anticancer drug delivery to tumour tissues.

5 CS/GA system

5.1 Unloaded CS/GA nanoparticles

Different chitosan and gum arabic concentrations, as well as their CS/GA concentration ratio and CS molecular weight were tested in order to define favourable formulations for the nanoparticles produced by polyelectrolyte conjugation of chitosan and gum arabic.

The formation of CS/GA nanoparticles occurred upon the dropwise addition of this negatively charged polysaccharide into the chitosan solution. An alteration on the solution from clear to opalescent was noticed, which indicates a change on the chitosan physical state to form nanoparticles when this polyelectrolyte complexation by ionic gelation method occurs.

5.1.1 Size and zeta potential characterization

The results of the sizes, polydispersity index and zeta potential of the produced nanoparticles are presented on Table 7 and Figure 6.

Table 7 – Physicochemical characterization of CS248/GA nanoparticles. Data represented as mean ± SD (n=3)

Ratio CS/GA	|CS| ($mg.mL^{-1}$)	|GA| ($mg.mL^{-1}$)	Mean diameter (nm)	PdI	ZP (mV)
0.75	0.3	0.4	386 ± 5	0.3 ± 0.2	50 ± 1
1.00	0.3	0.3	333 ± 3	0.3 ± 0.1	51 ± 1
1.50	0.3	0.2	322 ± 3	0.3 ± 0.1	51 ± 1
0.75	0.6	0.8	406 ± 3	0.3 ± 0.1	49 ± 1
1.00	0.6	0.6	342 ± 4	0.3 ± 0.2	52 ± 1
1.50	0.6	0.4	353 ± 3	0.3 ± 0.2	53 ± 1

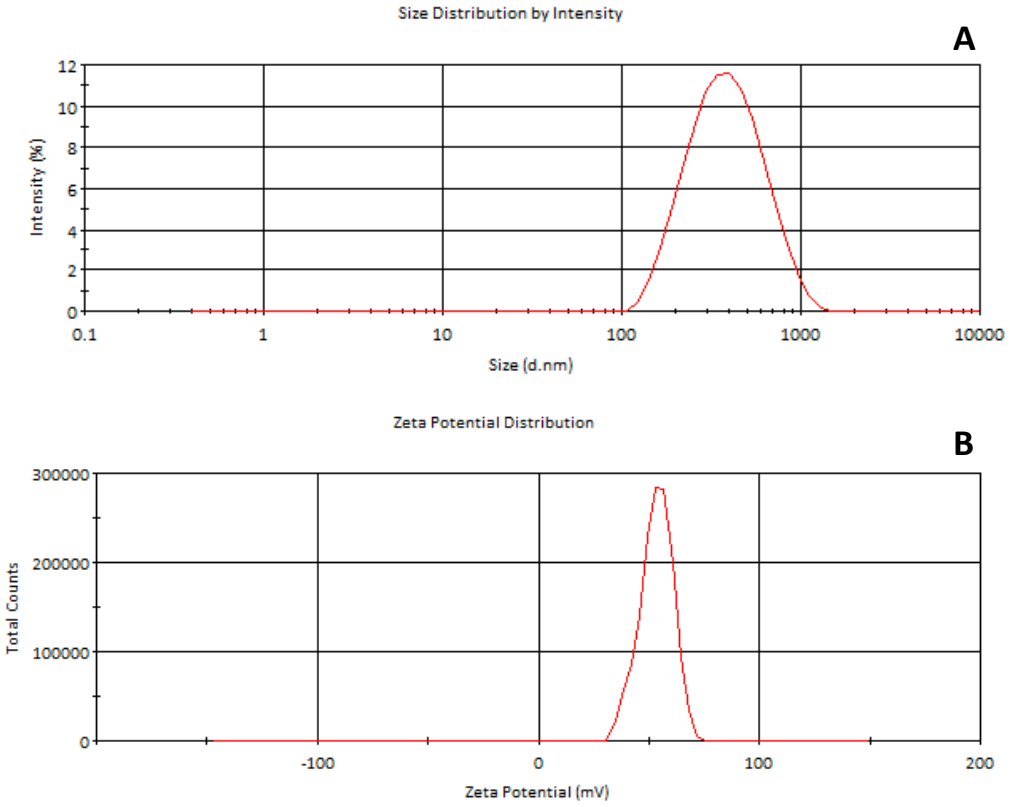

Figure 6 – Average hydrodynamic diameter distribution of CS248/GA NPs (CS 0.3:GA 0.4 mg.mL^{-1}) as determined by DLS (A) and zeta potential (B).

The CS/GA formulations prepared presented a mean diameter range between 322-406 nm, with a narrow size distribution (PdI = 0.3) and a zeta potential range of 49-53 mV. It can be concluded that the method followed for the preparation of CS/GA NPs produced well-stabilized monodisperse nanoparticles.

When comparing the different formulations with the same chitosan concentration, the size generally increased as the gum arabic concentration increases. As it is known, the complex is formed by electrostatic interactions between the carboxylic groups of arabic gum (-COO^-) and the amine groups of chitosan (-NH_3^+) (Espinosa-Andrews *et al.*, 2010; Coelho *et al.*, 2011). Thus, this size growth when GA concentration is higher possibly occurs due to the increased neutralized chitosan positive groups, which lowers the zeta potential and promotes attraction, which results in larger particle sizes. This tendency was visible in the range tested. To corroborate this theory, a slight and not significant ($P > 0.05$) decrease on zeta potential values when increasing GA concentrations was visible, since the higher the negative groups added to chitosan, the more the complexes tend towards electroneutrality. Besides, the addition of gum arabic into aqueous emulsions increase their viscosity, as it was reported by Wang and his co-workers (Wang *et al.*, 2011), which can be responsible for these physicochemical alterations.

Comparing the formulations using the same CS/GA ratios, a larger nanoparticle size was visible for the higher concentration chitosan (0.6 mg.mL^{-1}), although the mean diameters

were not significantly different ($P > 0.05$). As the GA concentration range was different in the two cases and the ones tested for the higher CS concentration are also higher, the noticed size increase was probably related to the increased GA concentration and, thus, direct conclusions cannot be taken. This increased mean diameter can be explained by the same presented theory, since a lower positive charge at the surface of the nanoparticles is also attained.

For the LMWC (CS20), the results obtained were slightly different, as it can be analysed in Table 8.

Table 8 – Physicochemical characterization of CS20/GA nanoparticles. Data represented as mean ± SD (n=3)

Ratio CS/GA	**|CS| ($mg.mL^{-1}$)**	**|GA| ($mg.mL^{-1}$)**	**Mean diameter (nm)**	**PdI**	**ZP (mV)**
0.75	0.3	0.4	473 ± 4	0.32 ± 0.1	32 ± 1
1.00	0.3	0.3	362 ± 4	0.26 ± 0.2	34 ± 1
1.50	0.3	0.2	303 ± 2	0.27 ± 0.1	32 ± 1
0.75	0.6	0.8	881 ± 12	0.60 ± 0.3	27 ± 1
1.00	0.6	0.6	532 ± 8	0.39 ± 0.2	28 ± 1
1.50	0.6	0.4	418 ± 5	0.27 ± 0.2	32 ± 1

The tendency of the size increase and the zeta potential decrease for increasing gum arabic concentrations was maintained from the MMWC. However, a general comparison of the physicochemical properties when using both molecular weight chitosans showed a higher mean diameter, although it is not significantly different ($P > 0.05$) and a very significantly ($P < 0.001$) diminished ZP of the CS20/GA nanoparticles.

Comparing the formulations using the same CS/GA ratios, a larger nanoparticle size and a lower zeta potential value are also visible for the higher concentration chitosan (0.6 $mg.mL^{-1}$) nanoparticles, although they also present the highest GA concentrations. Moreover, for the higher chitosan concentration, a strong instability of the produced nanoparticles can be perceived, especially for the ratio 0.75, where the highest CS and GA concentrations were tested, attaining a too high diameter and size distribution. This can be due to the shrinkage of the complexes when a large number of carboxylic groups interact with amine groups, resulting in the lowering of the nanoparticles' surface charge and intramolecular repulsion, which leads to the production of aggregates.

The chosen conditions to the subsequent experiments were the 0.75 with CS concentration of 0.3 $mg.mL^{-1}$ and the 1.5 also with the lowest CS concentration for the chitosan of molecular weight 248 and 20 kDa, respectively.

5.1.2 Morphologic analysis

The morphologic examination of the nanoparticles was performed by TEM. The obtained images of the unloaded CS/GA of the picked formulations for both MMWC and LMWC nanoparticles are shown in Figure 7.

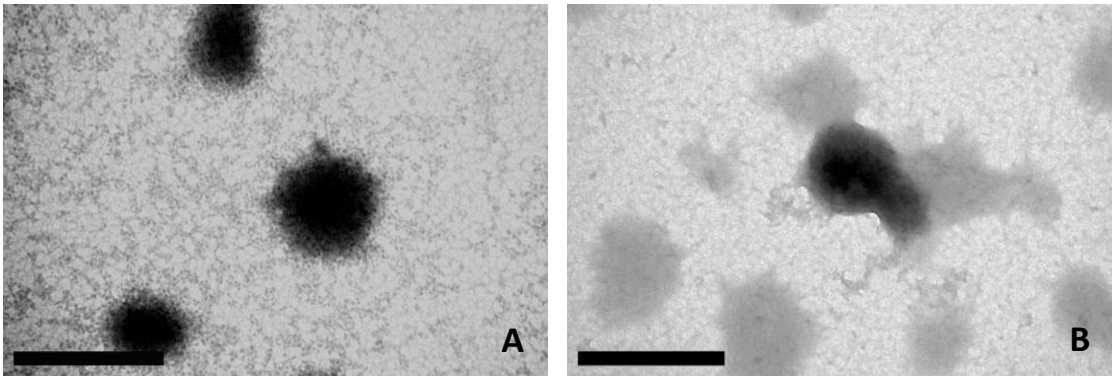

Figure 7 – TEM micrographs of free: (A) CS248/GA and (B) CS20/GA nanoparticles (The scale bar corresponds to 400 nm).

TEM analysis of these free CS/GA nanoparticles revealed a relatively spherical shape with a solid dense structure of the nanoparticles, although the CS20/GA nanoparticles present a less defined physical shape. The diameter of the nanoparticles revealed by this method changes between approximately 250 and 450 nm, which is in conformity with the size measurement by DLS.

5.2 Gemcitabine-loaded CS/GA nanoparticles

5.2.1 Size, zeta potential and gemcitabine encapsulation efficiency

The size, polydispersity index and zeta potential values for the gemcitabine-entrapped CS/GA NPs are presented in Table 9, as well as the gemcitabine encapsulation efficiencies and loading capacities for both low and medium molecular weight chitosan.

Table 9 – Physicochemical characterization, gemcitabine encapsulation efficiency and loading capacity values for CS/GA nanoparticles. Data represented as mean ± SD (n=5)

CS molecular weight (kDa)	Mean diameter (nm)	PdI	ZP (mV)	EE (%)	LC (%)
248	308 ± 2	0.3 ± 0.2	48 ± 1	38 ± 4	10 ± 1
20	724 ± 11	0.7 ± 0.3	31 ± 1	36 ± 6	10 ± 2

When the gemcitabine is entrapped in the CS/GA nanoparticles using CS of 248 kDa, their mean diameter values significantly decreased ($P < 0.05$) when compared to the unloaded CS/GA nanoparticles. The positive charge of the chitosan nanoparticles indicates that only a small part of the amine groups was neutralized and, thus, these residual amine groups are available for interaction with the added drug, as it was already stated by Arias and his colleagues (Arias *et al.*, 2011). The polydispersity index values did not change significantly ($P > 0.05$) before and after adding the drug to the nanoparticles either. The encapsulation efficiency and loading capacity attained were of medium extent and not significantly different ($P > 0.05$) between the two molecular weight chitosans. However, the low molecular weight chitosan particles have shown aggregates, evidenced by the aqueous suspension physical appearance, the too high mean diameters, high size distribution and low zeta potential values, when adding the drug. This fact led to the selection of the chitosan of 248 kDa for the following studies (CS248 is now referred to as just CS).

The coating of the nanoparticles' surface with polysorbate 80 was also studied, varying its concentration from 0.2 to 1% (v/v), being the physicochemical characterization of the uncoated and coated particles, as well as the entrapment and loading efficiencies of the drug on these systems presented on Table 10.

Table 10 – Physicochemical characterization, gemcitabine encapsulation efficiency and loading capacity values for CS/GA-Gem NPs coated by polysorbate 80 at different concentrations. Data represented as mean ± SD (n=3)

p80 concentration (% v/v)	Mean diameter (nm)	PdI	ZP (mV)	EE (%)	LC (%)
0	308 ± 2	0.3 ± 0.2	48 ± 1	38 ± 4	10 ± 1
0.20	274 ± 1	0.3 ± 0.3	45 ± 1	39 ± 3	18 ± 2
1.0	278 ± 1	0.4 ± 0.3	48 ± 2	66 ± 8	10 ± 0.2

The addition of polysorbate 80 results in a decreased size, which can be explained by the formation of a gel, leading to lesser water uptake, which causes smaller swelling, as stated by Hosseinzadeh and co-workers (Hosseinzadeh *et al.*, 2012), although mean diameters are not significantly different ($P > 0.05$). However, when carefully analysing Table 10, a small and not significant increase ($P > 0.05$) in the mean diameter and in the zeta potential is noticed between the addition of 0.2% and 1% p80 concentration. This fact can be due to a saturation of the association between this stabilizing agent to chitosan nanoparticles, since it is a nonionic highly viscous liquid. In fact, there are some FTIR studies reporting the competition between surfactants just as pluronic F-127 with gemcitabine for the interaction sites with chitosan molecules (Hosseinzadeh *et al.*, 2012). However, the encapsulation efficiency and the loading

capacity of gemcitabine-loaded nanoparticles is very significantly enhanced ($P < 0.001$) in the presence of polysorbate 80, especially at the concentration of 1% (v/v), being the difference in the presence of 0.2 and 1% polysorbate concentration significantly different ($P < 0.05$). There is no significant alteration ($P > 0.05$) in zeta potential values by adding p80, since it is a nonionic tensioactive. This not altered surface charge can also be explained by the mostly incorporation of the surfactant inside the nanoparticles matrix and not coated at the surface, as it was referred by Hosseinzadeh and co-workers when coating chitosan-gemcitabine nanoparticles with PF-127 (Hosseinzadeh *et al.*, 2012).

5.2.2 Morphologic analysis

TEM photographs of the gemcitabine-loaded CS/GA nanoparticles in the absence and in the presence of polysorbate 80 are shown in Figure 8.

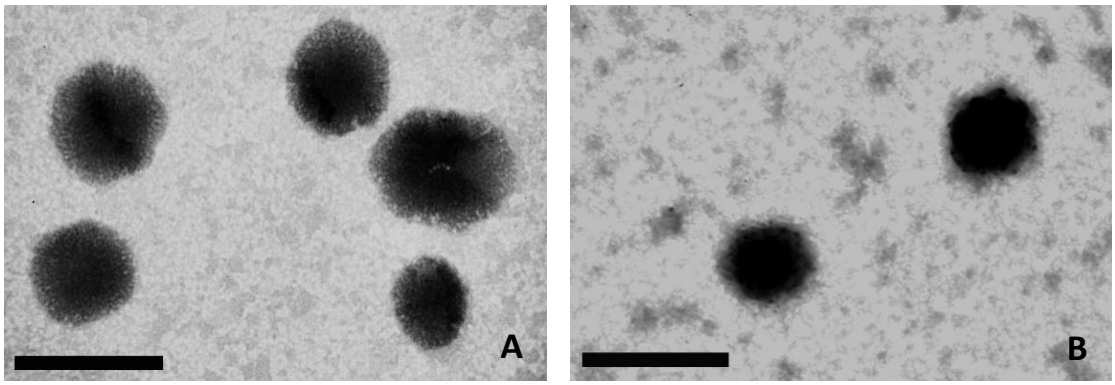

Figure 8 – TEM micrographs of gemcitabine-loaded: (A) CS/GA nanoparticles and (B) CS/GA-p80 nanoparticles (The scale bar corresponds to 400 nm).

The TEM images show spherical shapes and a relatively monodisperse nanoparticles. The presence of polysorbate 80 stabilizes the nanoparticle surface, as it had already been concluded in the physicochemical characterization of these particles and can be confirmed by the comparison of the figures A and B.

5.2.3 Process yield determination

The yield process was determined for the CS/GA-Gem and polysorbate 80-coated CS/GA-Gem nanoparticles.

The process yields attained were the ones presented in Table 11.

Table 11 – Process yields of CS/GA and p80-coated CS/GA nanoparticles

	Process yield (%)
CS/GA	49.5
CS/GA+p80	46.8

Although the addition of polysorbate 80 has resulted in higher encapsulation efficiencies, the same has not occurred with the process yield, having this value lowered when compared to the uncoated CS/GA nanoparticles. However, this difference is not statistically significant ($P > 0.05$).

5.2.4 Gemcitabine release from the nanoparticles

The dialysis method was used to evaluate the release profile of gemcitabine when free and in the prepared CS/GA nanoparticles. These release experiments were carried either in ultrapure water at 25 °C (results shown in Figure 9) and in phosphate buffered saline at 37 °C and pH 7.4 (Figure 10).

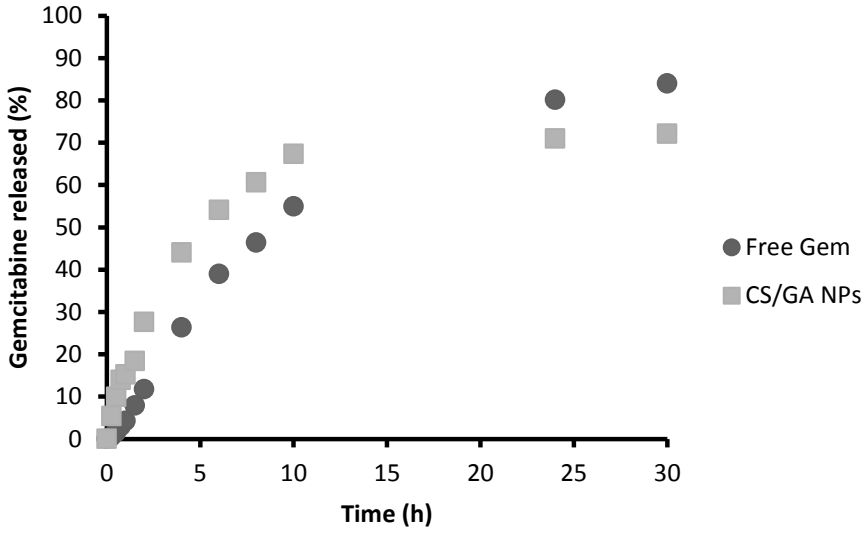

Figure 9 – Studies of gemcitabine release in water at 25 ± 1 °C free and entrapped in CS/GA NPs.

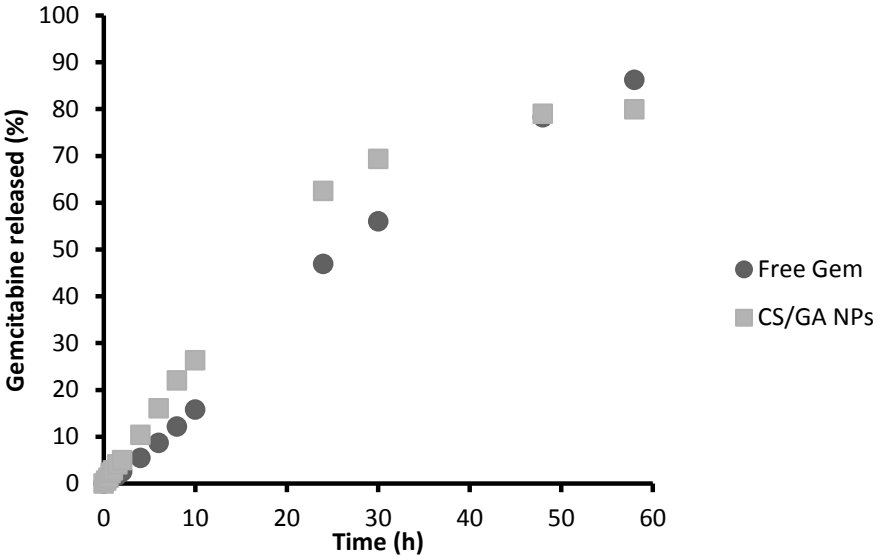

Figure 10 – Studies of gemcitabine release in PBS at pH 7.4 at 37 ± 1 °C free and entrapped in CS/GA NPs.

These *in vitro* experiments provide a guidance to predict the possible release profile of the drug when in the designed drug carriers. The *in vitro* gemcitabine release profile when in CS/GA nanoparticles showed a biphasic pattern with a rapid burst release followed by a slower sustained release of gemcitabine. The initial fast release (till the approximately 62-65% of gemcitabine released) might be due to the release of the free gemcitabine in solution or the one adsorbed to the NP surface, being the gemcitabine entrapped inside the core of NPs released in a later and more controlled manner. Several studies that developed CS nanoparticles for the encapsulation of gemcitabine have reported similar release profiles from the nanocarriers in PBS at 37 °C. Hosseinzadeh and his work partners (Hosseinzadeh *et al.*, 2012) have shown a burst drug release of almost 80% from CS nanoparticles at the end of 6 hours and a steady-state release of approximately 85% after 72 hours, attaining a lower release rate from CS with Pluronic F-127 nanoparticles. The gemcitabine release from CS nanoparticles reported by Arya and co-workers (Arya *et al.*, 2011) attained values of approximately 35% at the end of 24 hours and of 50% in the next 7 days. Arias and colleagues (Arias *et al.*, 2011), in turn, reached 40% of gemcitabine release in 2 hours and 60% at the end of 8 h, being the remaining encapsulated drug released over the next 4 days in a sustained way.

By comparing Figure 9 with Figure 10, the rapid release was especially visible in the case of water as the receiving phase (almost 70% of drug released in the first 10 h), when compared to the release in PBS (≈ 26% at the end of 10 hours). However, the release profile difference between the two receiving phases and between gemcitabine when free and when in nanoparticles was not significantly different ($P > 0.05$). Nevertheless, more assays must be carried in order to compare and conclude about precise release profiles in these different

conditions. The difference between the release profiles of gemcitabine in different media can be due to its properties. Avadi and his co-workers (Avadi *et al.*, 2010) have run release assays of insulin from chitosan/gum arabic nanoparticles in HCl at pH 1.2 and in PBS at pH 6.5 and pH 7.2 and revealed very different release profiles. They explained the observed burst release of insulin in acidic pH (90% at 1 hour) by the solubility of both chitosan and insulin and the difference between release in PBS at pH 6.5 and 7.2 (≈ 35% and 80% at the end of 7 hours, respectively) by the gum arabic properties. They defend that the chains of arabic gum in media with pH higher than 6.5 tend to swell and disturb the structure of nanoparticles, which leads to a higher porosity in the nanoparticle structure and enhances the drug release rate.

The size, solubility, composition and biodegradation of the nanoparticle matrix are the main factors that affect the release rate of a drug from nanoparticles (Kumari *et al.*, 2010). Desai (Desai, 2012) stated that the intentional designed nanocarriers with mixed sizes has been proposed in order to attain a drug release in a sustained manner over time. Besides, a time compromise in the drug release profile is needed, since if the gemcitabine-loaded NPs present a too high stability, the drug liberation will not occur when the particles are targeted, and if the drug is not well entrapped, it can lead to premature and not favourable gemcitabine release. It can be concluded that the developed CS/GA nanosystem is a favourable approach for the gemcitabine transport and release, due to its biphasic and controlled pattern.

5.2.5 Cytotoxicity studies

The *in vitro* cytotoxic effects on a pancreatic cancer cell line upon its treatment with gemcitabine entrapped into the prepared CS/GA and polysorbate 80-coated CS/GA nanoparticles were assessed, comparatively to the free drug, in terms of cell survival and growth. Bare CS/GA(+p80 0.20) nanoformulations have shown no deleterious effect on cell viability in this human pancreatic cell line (Figure 11).

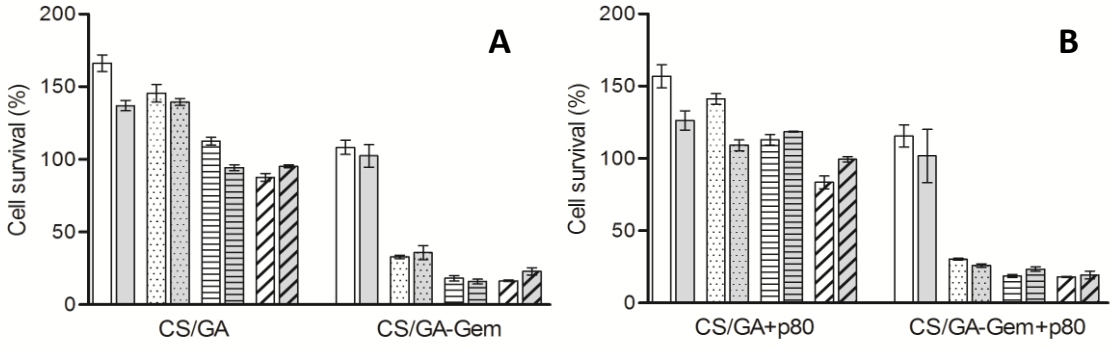

Figure 11 – Cell survival after 48 h exposure to bare and gemcitabine-loaded NPs of CS/GA (A) and CS/GA+p80 (B) (mean of three replicates per treatment ± SEM). Gemcitabine concentrations of the depicted NPs are 5, $1x10^2$, $1x10^3$ and $1x10^4$ nM; the bare NPs were tested at dilutions analogous to the NPs loaded with gemcitabine. White coloured bars show results obtained with PB assay; grey coloured bars show results obtained with SRB assay.

The CS/GA(+p80) formulations with gemcitabine showed a gemcitabine concentration-related decrease in cell survival and growth after 48 h of exposure (Figure 12 for PB assay and Figure 13 for SRB assay).

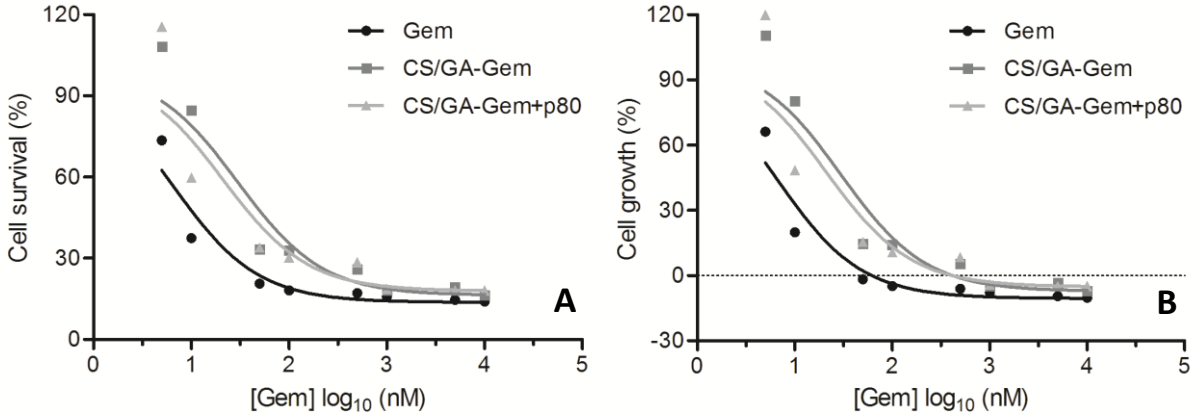

Figure 12 – Cytotoxic effects of gemcitabine free and entrapped in CS/GA and CS/GA+p80 NPs on a human pancreatic cell line, determined by PrestoBlue™ assay: (A) effects of gemcitabine on cell survival; (B) effects of gemcitabine on cell growth.

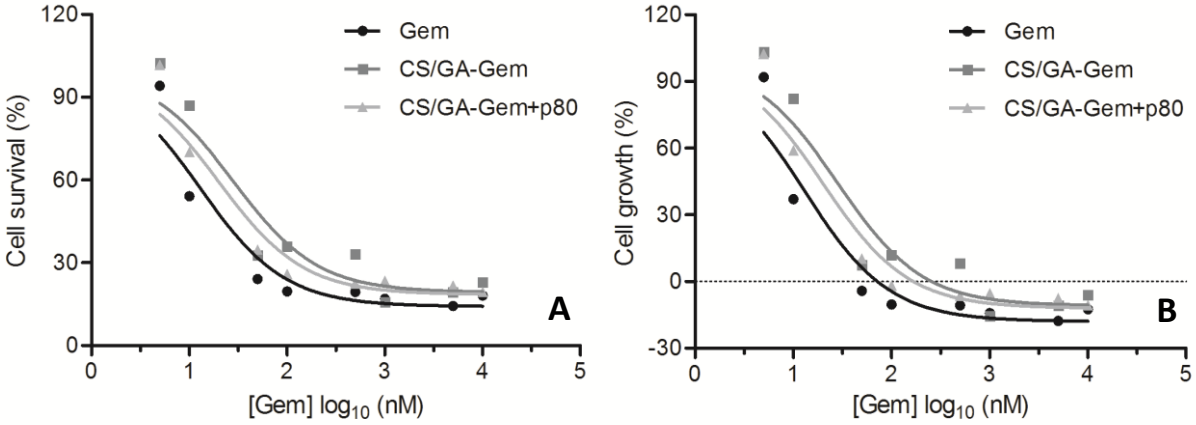

Figure 13 – Cytotoxic effects of gemcitabine free and entrapped in CS/GA and CS/GA+p80 NPs on a human pancreatic cell line, determined by Sulforhodamine B assay: (A) effects of gemcitabine on cell survival; (B) effects of gemcitabine on cell growth.

The attained results (Table 12) showed that free gemcitabine presents the lowest IC_{50} and GI_{50} values. Nonetheless, CS/GA and p80-coated CS/GA nanoparticles loaded with gemcitabine were also effective at decreasing cell survival and inhibiting cell growth.

Table 12 – Cytotoxic effects of gemcitabine on the survival and growth of a human pancreatic tumour cell line. Results are expressed as IC_{50} and GI_{50} at 48 h of exposure with respective 95% Confidence Limits for gemcitabine free and entrapped in CS/GA and CS/GA+p80 NPs and by PB and SRB assays

	IC_{50} (nM)		**GI_{50} (nM)**	
	PB	SRB	PB	SRB
Gem	8.9 (7.0 – 11.2)	18.0 (12.2 – 25.9)	5.4 (5.0 – 6.8)	9.5 (6.5 – 14.0)
CS/GA-Gem	44.2 (29.6 – 64.1)	45.7 (28.8 – 68.9)	26.1 (17.6 – 38.6)	23.1 (14.9 – 35.9)
CS/GA-Gem+p80	33.1 (18.7 – 54.6)	32.0 (18.5 – 51.8)	19.2 (11.2 – 32.8)	16.3 (9.7 – 27.4)

The IC_{50} and GI_{50} values attained by following both methodologies (PB and SRB) are concordant with each other, since they are not significantly different ($t = 0.88$, df = 8, $P > 0.05$; $t = 0.84$, df = 8, $P > 0.05$, for IC_{50} and GI_{50} values, respectively). These quantitative results show that gemcitabine free is significantly more effective at decreasing cell survival and inhibiting cell growth, as it presents the lowest IC_{50} and GI_{50} values ($F = 13.17$, df = 2.15, $P < 0.05$; $F = 9.88$, df = 2.15, $P < 0.05$, respectively), in comparison with CS/GA-Gem(+p80) treatments, that need a higher gemcitabine concentration to reach the same effect. Though not with a significant difference, it is also visible that the IC_{50} and, consequently, GI_{50} values decreased by the surface-coating of the nanoparticles with polysorbate 80, indicating an increased cytotoxic effect upon the addition of p80. In fact, Tukey's multiple comparison tests have shown that the IC_{50} and GI_{50} values of free gemcitabine were significantly different from the gemcitabine when entrapped in CS/GA(+p80) ($P < 0.05$) but between CS/GA-Gem and CS/GA-Gem+p80 nanoparticles there was no statistical difference ($P > 0.05$).

These results can possibly be explained by the controlled release of the drug when carried by the nanosystems after cellular uptake, which leads to a more prolonged therapeutic effect. As it is evident from the release profile of the nanoparticle formulation (Figure 10), the surface-adsorbed gemcitabine is rapidly released, but the entrapped drug is released in a lower sustained manner. Sloat and his co-workers (Sloat *et al.*, 2011) have shown lower cytotoxic effect of the prepared nanoparticles incorporating gemcitabine derivative GemC18 than the free gemcitabine HCl. However, when the incubation time of the tumour cells treated with GemC18 nanoparticles was increased for 48 hours, the percentage of dead cells reached was similar to the one attained for free gemcitabine for 24 h incubation time. This occurrence indicates that it was just a question of time for the GemC18-loaded nanoparticles to kill tumour cells, also explained by the slow release of gemcitabine. Therefore, the total amount of the drug present in cancer

cells is possibly a combination of the free or surface-adsorbed drug and the encapsulated gemcitabine in the core of the nanoparticles.

As it was mentioned before, gemcitabine requires mediated transport to enter the cells by membrane proteins called nucleoside transporters, since it is a hydrophilic low-molecular-weight anticancer drug, which is a selective and saturable process (Reddy *et al.*, 2007). By intravenous via, absorption process is absent, since the pharmaceutical compound directly enters the blood circulation, reaching maximal plasmatic concentrations right after its administration. However, when intravenously injected, free gemcitabine undergoes rapid deamination by the enzyme cytidine deaminase into the inactive uracil derivative (dFdU), which results in a rapid metabolism and short half-time. When inside the cells, gemcitabine is primarily phosphorylated by deoxycytidine kinase into its active metabolite, gemcitabine monophosphate, and consequently diphosphate and triphosphate (Reddy *et al.*, 2007; Hosseinzadeh *et al.*, 2012).

The rapid release of adsorbed-gemcitabine from the nanostructures in the extracellular media increases the free drug availability for entrance in the cells through membrane transporters, while the nanoparticles with gemcitabine in their core are endocytosed by the cells, a process mediated by clathrin (Hosseinzadeh *et al.*, 2012). Some studies have already referred the higher therapeutic concentration and increased cytotoxicity of gemcitabine when the cancer cell uptake is made by both transport pathways (Trickler *et al.*, 2010; Hosseinzadeh *et al.*, 2012). Besides, the entrapment of gemcitabine into the chitosan/gum arabic nanoparticles protects and prevents the drug from degradation by the cytidine-deaminase enzyme and its rapid metabolization during intravenous administration, increasing its half-life. Therefore, the overcoming of the actual limitations will lead to a higher bioavailability and lower doses of gemcitabine needed, which, in turn, contributes to the increased therapeutic efficacy at the specific tumour targets.

Although higher IC_{50} and GI_{50} values were obtained for the gemcitabine-loaded CS/GA(+p80) nanoparticles, when compared to the administered free drug, the developed formulation present the several referred advantages and the attained results encourage the use of these nanocarriers for the targeted delivery of this anticancer drug. However, further studies must be carried to analyse and elucidate the *in vitro* and *in vivo* cytotoxicity of the gemcitabine-loaded nanoparticles, cell uptake mechanisms, intracellular routes, as well as mucoadhesion and pharmacokinetic investigation.

6 Conclusions and Future Perspectives

6.1 Conclusions

New approaches are being extensively studied and investigated for the anticancer drug delivery to tumour cells, since there are several limitations and side effects associated with the traditional cancer treatment methods. Nanoparticles have appeared as promising candidates for the development of an anticancer drug delivery system, presenting numerous advantages over conventional chemotherapy such as improving the drug water solubility, protecting it from the macrophage uptake, thus enhancing the blood circulation time, and finally providing an increased and controlled release into the specific final target.

Polysaccharide-based nanoparticles, in particular, present several favourable properties besides the permission for the chemotherapeutic drugs to be effectively delivered into specific tumour cells, related to the water solubility, biocompatibility and biodegradability properties of these polymers. Although significant progress on the polysaccharide-based systems for the anticancer drug delivery has been made during the last years, an ideal carrier has not yet been achieved. Some nanoparticles were also developed to entrap gemcitabine, a highly soluble low-molecular-weight anticancer drug with a short plasma half-life, in order to improve its bioavailability and increase its therapeutic efficacy in specific tumour cells.

In this work, chitosan-based nanoparticles were prepared by ionic gelation upon the addition of a negatively charged polymer. A detailed physicochemical and morphologic characterization using several varying parameters such as chitosan molecular weight, polymers concentration and their mass concentration ratio allowed to define the optimal nanoparticles formulation conditions suitable for the gemcitabine encapsulation and delivery into tumour cells.

Chitosan nanoparticles were immediately produced upon the dropwise addition of tripolyphosphate by the formed ionic crosslinking between the negatively charged phosphate groups of TPP and the protonated amine groups of chitosan. Gemcitabine-loaded nanoparticles were produced using the conditions that were concluded to be the most favourable ones and presented a mean diameter of approximately 370 nm, as well as a positive zeta potential. However, these nanoparticles were difficult to separate by centrifugation, which turned it impossible to determine the encapsulation efficiency of the drug. This was the main reason for the abandonment of this formulation, in conjunction with the suspected crystallization phenomena of these nanoparticles, visible by TEM micrographs, and focus on the alternative proposal.

Chitosan/gum arabic nanoparticles were prepared by polyelectrolyte complexation when electrostatic interactions between the negatively charged carboxylic groups of gum arabic and the amine groups of chitosan occur. The physicochemical characterization allowed the determination of the most adequate conditions for the encapsulation and delivery of gemcitabine. These CS/GA nanoparticles presented a size of approximately 300 nm, low level of size distribution, positive zeta potential and a spherical shape, shown by TEM images. The encapsulation of 12.5% (w/w) of gemcitabine reached values of efficiency of approximately 38% and loading capacity of 10%, being the attained drug entrapment process yield of about 50%. These are medium satisfactory results that could be enhanced, possibly by varying polymers mass, gemcitabine concentration or other production conditions, in order to reduce the quantity of the carrier required for the drug administration. When these nanoparticles were coated with polysorbate 80, a size decrease and an increase in the gemcitabine encapsulation percentage occurred, which, together with the morphologic analysis by TEM, proved its stabilizing effect on the nanoparticles.

The release profile of gemcitabine when in the nanoparticles was similar to the attained for the free drug till the 62% of gemcitabine was released, which may be correspondent to the free or surface-adsorbed drug, followed by a slower sustained release phase, attributed to the entrapped gemcitabine in the core of the NPs. The concentration-response studies on cancer cells revealed a higher cytotoxicity of the free gemcitabine, although CS/GA-Gem NPs have also shown cytotoxic effect, which can possibly be due to a later effect, suspicion based on the sustained-release of the entrapped gemcitabine. Despite of the higher IC_{50} value obtained for the gemcitabine-loaded CS/GA nanoparticles, when compared to the free drug, this formulation presents the enormous advantage of drug protection and prevention from degradation, increasing gemcitabine half-life and of the existence of two parallel transport pathways for the gemcitabine controlled release. Besides the enhanced drug bioavailability, it is believed that this formulation exhibits better selectivity for target cancer cells and tissues, in comparison with free drug, which results in a higher therapeutic efficiency.

Overall, the attained results suggest that this CS/GA nanosystem, prepared by a rapid and mild procedure without using organic solvents, can be considered a good candidate for the targeted delivery of the anticancer drug gemcitabine in the treatment of pancreatic cancer, possibly allowing lower doses to be administered.

6.2 Future perspectives

There are several experiences and tests that, throughout the work, had been interesting but were not possible to be performed due to time restrictions. It would be important to explore the ideal CS/TPP-Gem nanoparticles production conditions and find the adequate centrifugation conditions, or an alternative separation methodology if it kept impossible to determine the gemcitabine entrapment efficiency, loading capacity and process yield.

The developed CS/GA nanoparticles have proved to be a promising new approach to address gemcitabine to specific cancer cells, although further investigation is required, in order to optimize, clarify and support the advantages of this formulation. Some studies on the chitosan/gum arabic nanoparticles characterization and evaluation when varying the pH and the temperature would be interesting to be performed, as well as a stability study, in order to clarify and fully characterize their behaviour at different medium conditions and for long periods. Many other parameters such as the gemcitabine loaded concentration or the polysorbate 80 concentration could be varied in order to analyse the formed nanoparticles' physicochemical characteristics and reaching the maximal gemcitabine loading capacity, entrapment efficiency and process final yield. FTIR, NMR and DSC studies should also be carried in order to investigate the gemcitabine entrapment into the nanoparticles, their chemical characterization and the physical state of the drug when inside the nanoparticles, respectively.

In order to elucidate the presence of two different release phases, the release profiles should be performed for all the formulations tested, since they are responsible for the belief that there are two simultaneous transport mechanisms for the gemcitabine entrance into cancer cells. Additionally, a more detailed study for the better understanding of the nanoparticles' cell uptake, intracellular routes and their destination must be performed, in order to ascertain their specificity and safety for the controlled-delivery purpose. The conjugation of a specific ligand or an epidermal growth factor receptor could also be tested, in order to enable molecular recognition and achieve specific targeting to pancreatic cancer cells.

To evolve through later stages of investigation, *in vivo* anti-tumour tests with mice, pharmacokinetics and mucoadhesion studies, biodistribution of gemcitabine in tumour-bearing

mice and histological observation of the treated tumours must be aimed, apart from the study of more practical issues such as costs and manufacturability.

7 References

Agnihotri, S. A., Mallikarjuna, N. N.,Aminabhavi, T. M. (2004). *Recent advances on chitosan-based micro- and nanoparticles in drug delivery*. J Control Release 100(1): 5-28.

Al-Qadi, S., Grenha, A.,Remuñán-López, C. (2011). *Microspheres loaded with polysaccharide nanoparticles for pulmonary delivery: Preparation, structure and surface analysis*. Carbohydrate Polymers 86(1): 25-34.

Alonso-Sande, M., Cuña, M., Remuñán-López, C., Teijeiro-Osorio, D., Alonso-Lebrero, J. L.,Alonso, M. J. (2006). *Formation of new glucomannan-chitosan nanoparticles and study of their ability to associate and deliver proteins*. Macromolecules 39(12): 4152-4158.

Annarita, P., Paola, D. D., Gennaro Roberto, A.,Barbara, N. (2011). *Synthesis, Production, and Biotechnological Applications of Exopolysaccharides and Polyhydroxyalkanoates by Archaea*. Archaea 2011.

Arias, J. L., Reddy, L. H.,Couvreur, P. (2008). *Magnetoresponsive squalenoyl gemcitabine composite nanoparticles for cancer active targeting*. Langmuir 24(14): 7512-7519.

Arias, J. L., Reddy, L. H.,Couvreur, P. (2011). *Superior preclinical efficacy of gemcitabine developed as chitosan nanoparticulate system*. Biomacromolecules.

Arya, G., Vandana, M., Acharya, S.,Sahoo, S. K. (2011). *Enhanced antiproliferative activity of Herceptin (HER2)-conjugated gemcitabine-loaded chitosan nanoparticle in pancreatic cancer therapy*. Nanomedicine: Nanotechnology, Biology and Medicine.

Avadi, M., Sadeghi, A., Dounighi, N. M., Dinarvand, R., Atyabi, F.,Rafiee-Tehrani, M. (2011). *Ex Vivo Evaluation of Insulin Nanoparticles Using Chitosan and Arabic Gum*. ISRN Pharmaceutics 2011.

Avadi, M. R., Sadeghi, A. M. M., Mohammadpour, N., Abedin, S., Atyabi, F., Dinarvand, R.,Rafiee-Tehrani, M. (2010). *Preparation and characterization of insulin nanoparticles using chitosan and Arabic gum with ionic gelation method*. Nanomedicine: Nanotechnology, Biology and Medicine 6(1): 58-63.

Barreto, J. A., O'Malley, W., Kubeil, M., Graham, B., Stephan, H.,Spiccia, L. (2011). *Nanomaterials: applications in cancer imaging and therapy*. Adv Mater 23(12): H18-40.

Bodnar, M., Hartmann, J. F.,Borbely, J. (2005). *Preparation and characterization of chitosan-based nanoparticles*. Biomacromolecules 6: 2521-2527.

Burris, H. A., Moore, M. J., Andersen, J., Green, M. R., Rothenberg, M. L., Modiano, M. R., Cripps, M. C., Portenoy, R. K., Storniolo, A. M.,Tarassoff, P. (1997). *Improvements in survival and clinical benefit with gemcitabine as first-line therapy for patients with advanced pancreas cancer: a randomized trial*. Journal of clinical oncology 15(6): 2403-2413.

Cahn, R. W.,Haansen, P. (1996). Physical Metallurgy, Volume 2, Elsevier North Holland.

Calvo, P., Remuñán-López, C., Vila-Jato, J. L.,Alonso, M. J. (1997). *Novel hydrophilic chitosan-polyethylene oxide nanoparticles as protein carriers*. Journal of Applied Polymer Science 63(1): 125-132.

Chavanpatil, M. D., Khdair, A.,Panyam, J. (2007). *Surfactant-polymer nanoparticles: a novel platform for sustained and enhanced cellular delivery of water-soluble molecules*. Pharm Res 24(4): 803-810.

Chen, Y., Mohanraj, V. J., Wang, F.,Benson, H. A. E. (2007). *Designing chitosan-dextran sulfate nanoparticles using charge ratios*. AAPS PharmSciTech 8(4): 131-139.

Cho, K., Wang, X., Nie, S., Chen, Z. G.,Shin, D. M. (2008). *Therapeutic nanoparticles for drug delivery in cancer*. Clin Cancer Res 14(5): 1310-1316.

Choi, K. Y., Saravanakumar, G., Park, J. H.,Park, K. (2011). *Hyaluronic Acid-Based Nanocarriers for Intracellular Targeting: Interfacial Interactions with Proteins in Cancer*. Colloids and Surfaces B: Biointerfaces.

Coelho, S., Moreno-Flores, S., Toca-Herrera, J. L., Coelho, M. A. N., Pereira, M. C.,Rocha, S. (2011). *Nanostructure of polysaccharide complexes*. Journal of colloid and interface science.

Csaba, N., Köping-Höggård, M.,Alonso, M. J. (2009). *Ionically crosslinked chitosan/tripolyphosphate nanoparticles for oligonucleotide and plasmid DNA delivery*. Int J Pharm 382(1): 205-214.

Desai, N. (2012). *Challenges in Development of Nanoparticle-Based Therapeutics*. The AAPS journal: 1-14.

Duncan, R. (2006). *Polymer conjugates as anticancer nanomedicines*. Nat Rev Cancer 6(9): 688-701.

Earhart, C., Jana, N. R., Erathodiyil, N.,Ying, J. Y. (2008). *Synthesis of Carbohydrate-Conjugated Nanoparticles and Quantum Dots*. Langmuir 24: 6215-6219.

Espinosa-Andrews, H., Báez-González, J. G., Cruz-Sosa, F.,Vernon-Carter, E. J. (2007). *Gum Arabic−Chitosan Complex Coacervation*. Biomacromolecules 8(4): 1313-1318.

Espinosa-Andrews, H., Sandoval-Castilla, O., Vázquez-Torres, H., Vernon-Carter, E. J.,Lobato-Calleros, C. (2010). *Determination of the gum Arabic–chitosan interactions by Fourier Transform Infrared Spectroscopy and characterization of the microstructure and rheological features of their coacervates*. Carbohydrate Polymers 79(3): 541-546.

Fang, N., Chan, V., Mao, H.-Q.,Leong, K. W. (2001). *Interactions of phospholipid bilayer with chitosan: Effect of molecular weight and pH*. Biomacromolecules 2: 1161-1168.

Felt, O., Buri, P.,Gurny, R. (1998). *Chitosan: a unique polysaccharide for drug delivery*. Drug Development and Industrial Pharmacy 24: 979-993.

Feng, S.-S.,Chien, S. (2003). *Chemotherapeutic engineering: Application and further development of chemical engineering principles for chemotherapy of cancer and other diseases*. Chemical Engineering Science 58(18): 4087-4114.

Gabas, A. L., Telis, V. R. N., Sobral, P. J. A.,Telis-Romero, J. (2007). *Effect of maltodextrin and arabic gum in water vapor sorption thermodynamic properties of vacuum dried pineapple pulp powder*. Journal of Food Engineering 82(2): 246-252.

Gan, Q., Wang, T., Cochrane, C.,McCarron, P. (2005). *Modulation of surface charge, particle size and morphological properties of chitosan–TPP nanoparticles intended for gene delivery*. Colloids and Surfaces B: Biointerfaces 44(2): 65-73.

Gang, J., Park, S. B., Hyung, W., Choi, E. H., Wen, J., Kim, H. S., Shul, Y. G., Haam, S.,Song, S. Y. (2007). *Magnetic poly ϵ-caprolactone nanoparticles containing Fe3O4 and gemcitabine enhance anti-tumor effect in pancreatic cancer xenograft mouse model*. Journal of drug targeting 15(6): 445-453.

Gomes, J. F. P. S., Rocha, S., Pereira, M. C., Peres, I., Moreno, S., Toca-Herrera, J.,Coelho, M. A. N. (2010). *Lipid/particle assemblies based on maltodextrin-gum arabic core as bio-carriers*. Colloids and Surfaces B: Biointerfaces 76(2): 449-455.

Gu, F. X., Karnik, R., Wang, A. Z., Alexis, F., Levy-Nissenbaum, E., Hong, S., Langer, R. S.,Farokhzad, O. C. (2007). *Targeted nanoparticles for cancer therapy*. Nano Today 2(3): 14-21.

Haley, B.,Frenkel, E. (2008). *Nanoparticles for drug delivery in cancer treatment*. Urol Oncol 26(1): 57-64.

Hans, M. L.,Lowman, A. M. (2002). *Biodegradable nanoparticles for drug delivery and targeting*. Current Opinions in Solid State and Materials Science 6: 319-327.

Hejazi, R.,Amiji, M. (2003). *Chitosan-based gastrointestinal delivery systems*. Journal of Controlled Release 89(2): 151-165.

Hosseinzadeh, H., Atyabi, F., Dinarvand, R.,Ostad, S. N. (2012). *Chitosan–Pluronic nanoparticles as oral delivery of anticancer gemcitabine: preparation and in vitro study*. International Journal of Nanomedicine 7: 1851.

Hu, B., Pan, C., Sun, Y., Hou, Z., Ye, H., Hu, B.,Zeng, X. (2008a). *Optimization of fabrication parameters to produce chitosan− tripolyphosphate nanoparticles for delivery of tea catechins*. Journal of Agricultural and Food Chemistry 56(16): 7451-7458.

Hu, F. Q., Wu, X. L., Du, Y. Z., You, J.,Yuan, H. (2008b). *Cellular uptake and cytotoxicity of shell crosslinked stearic acid-grafted chitosan oligosaccharide micelles encapsulating doxorubicin*. Eur J Pharm Biopharm 69(1): 117-125.

Hwang, H. Y., Kim, I. S., Kwon, I. C.,Kim, Y. H. (2008). *Tumor targetability and antitumor effect of docetaxel-loaded hydrophobically modified glycol chitosan nanoparticles*. Journal of Controlled Release 128(1): 23-31.

Hyung Park, J., Kwon, S., Lee, M., Chung, H., Kim, J. H., Kim, Y. S., Park, R. W., Kim, I. S., Bong Seo, S., Kwon, I. C.,Young Jeong, S. (2006). *Self-assembled nanoparticles based on glycol chitosan bearing hydrophobic moieties as carriers for doxorubicin: in vivo biodistribution and anti-tumor activity*. Biomaterials 27(1): 119-126.

Janes, K. A., Calvo, P.,Alonso, M. J. (2001). *Polysaccharide colloidal particles as delivery systems for macromolecules*. Adv Drug Deliv Rev 47: 83-97.

Kim, Y. D.,Morr, C. V. (1996). *Microencapsulation Properties of Gum Arabic and Several Food Proteins: Spray-Dried Orange Oil Emulsion Particles*. Journal of Agricultural and Food Chemistry 44(5): 1314-1320.

Kumari, A., Yadav, S. K.,Yadav, S. C. (2010). *Biodegradable polymeric nanoparticles based drug delivery systems*. Colloids Surf B Biointerfaces 75(1): 1-18.

Kurozawa, L. E., Park, K. J.,Hubinger, M. D. (2009). *Effect of maltodextrin and gum arabic on water sorption and glass transition temperature of spray dried chicken meat hydrolysate protein*. Journal of Food Engineering 91(2): 287-296.

Kwon, S., Park, J. H., Chung, H., Kwon, I. C., Jeong, S. Y.,Kim, I. S. (2003). *Physicochemical characteristics of self-assembled nanoparticles based on glycol chitosan bearing 5β-cholanic acid*. Langmuir 19(24): 10188-10193.

Ladaviere, C., Averlant-Petit, M. C., Fabre, O., Durand, A., Dellacherie, E.,Marie, E. (2007). *Preparation of polysaccharide-coated nanoparticles by emulsion polymerization of styrene*. Colloid and Polymer Science 285(6): 621-630.

Lee, E., Lee, J., Lee, I. H., Yu, M., Kim, H., Chae, S. Y.,Jon, S. (2008). *Conjugated chitosan as a novel platform for oral delivery of paclitaxel*. J Med Chem 51(20): 6442-6449.

Lemarchand, C., Gref, R.,Couvreur, P. (2004). *Polysaccharide-decorated nanoparticles*. Eur J Pharm Biopharm 58(2): 327-341.

Lemarchand, C., Gref, R., Lesieur, S., Hommel, H., Vacher, B., Besheer, A., Maeder, K.,Couvreur, P. (2005). *Physico-chemical characterization of polysaccharide-coated nanoparticles*. J Control Release 108(1): 97-111.

Lemarchand, C., Gref, R., Passirani, C., Garcion, E., Petri, B., Muller, R., Costantini, D.,Couvreur, P. (2006). *Influence of polysaccharide coating on the interactions of nanoparticles with biological systems*. Biomaterials 27(1): 108-118.

Li, F., Li, J., Wen, X., Zhou, S., Tong, X., Su, P., Li, H.,Shi, D. (2009). *Anti-tumor activity of paclitaxel-loaded chitosan nanoparticles: An in vitro study*. Materials Science and Engineering: C 29(8): 2392-2397.

Liu, Z., Jiao, Y., Wang, Y., Zhou, C.,Zhang, Z. (2008). *Polysaccharides-based nanoparticles as drug delivery systems*. Adv Drug Deliv Rev 60(15): 1650-1662.

Ma, W.-j., Yuan, X.-b., Kang, C.-s., Su, T., Yuan, X.-y., Pu, P.-y.,Sheng, J. (2008). *Evaluation of blood circulation of polysaccharide surface-decorated PLA nanoparticles*. Carbohydrate Polymers 72(1): 75-81.

Mackey, J. R., Mani, R. S., Selner, M., Mowles, D., Young, J. D., Belt, J. A., Crawford, C. R.,Cass, C. E. (1998). *Functional nucleoside transporters are required for gemcitabine influx and manifestation of toxicity in cancer cell lines*. Cancer research 58(19): 4349.

Malam, Y., Loizidou, M.,Seifalian, A. M. (2009). *Liposomes and nanoparticles: nanosized vehicles for drug delivery in cancer*. Trends Pharmacol Sci 30(11): 592-599.

McNamee, B. F., O'Riorda, E. D.,O'Sullivan, M. (1998). *Emulsification and Microencapsulation Properties of Gum Arabic*. Journal of Agricultural and Food Chemistry 46(11): 4551-4555.

Mitra, S., Gaur, U., Ghosh, P. C.,Maitra, A. N. (2001). *Tumour targeted delivery of encapsulated dextran–doxorubicin conjugate using chitosan nanoparticles as carrier*. Journal of Controlled Release 74: 317-323.

Morille, M., Passirani, C., Vonarbourg, A., Clavreul, A.,Benoit, J. P. (2008). *Progress in developing cationic vectors for non-viral systemic gene therapy against cancer*. Biomaterials 29(24-25): 3477-3496.

Moschakis, T., Murray, B. S.,Biliaderis, C. G. (2010). *Modifications in stability and structure of whey protein-coated o/w emulsions by interacting chitosan and gum arabic mixed dispersions*. Food Hydrocolloids 24(1): 8-17.

Mu, L.,Feng, S. (2001). *Fabrication, characterization and in vitro release of paclitaxel (Taxol®) loaded poly (lactic-co-glycolic acid) microspheres prepared by spray*

drying technique with lipid/cholesterol emulsifiers. Journal of Controlled Release 76(3): 239-254.

Na, K., Bum Lee, T., Park, K.-H., Shin, E.-K., Lee, Y.-B.,Choi, H.-K. (2003). *Self-assembled nanoparticles of hydrophobically-modified polysaccharide bearing vitamin H as a targeted anti-cancer drug delivery system*. European Journal of Pharmaceutical Sciences 18(2): 165-173.

Nie, S., Xing, Y., Kim, G. J.,Simons, J. W. (2007). *Nanotechnology applications in cancer*. Annu Rev Biomed Eng 9: 257-288.

Park, J. H., Lee, S., Kim, J. H., Park, K., Kim, K.,Kwon, I. C. (2008). *Polymeric nanomedicine for cancer therapy*. Progress in Polymer Science 33(1): 113-137.

Park, J. H., Saravanakumar, G., Kim, K.,Kwon, I. C. (2010). *Targeted delivery of low molecular drugs using chitosan and its derivatives*. Adv Drug Deliv Rev 62(1): 28-41.

Pastor-Anglada, M., Molina-Arcas, M., Casado, F., Bellosillo, B., Colomer, D.,Gil, J. (2004). *Nucleoside transporters in chronic lymphocytic leukaemia*. Leukemia 18(3): 385-393.

Peer, D., Karp, J. M., Hong, S., Farokhzad, O. C., Margalit, R.,Langer, R. (2007). *Nanocarriers as an emerging platform for cancer therapy.* Nature 2: 751-760.

Peres, I., Rocha, S., Pereira, M. C., Coelho, M., Rangel, M.,Ivanova, G. (2010). *NMR structural analysis of epigallocatechin gallate loaded polysaccharide nanoparticles*. Carbohydrate Polymers 82(3): 861-866.

Qiao, W., Wang, B., Wang, Y., Yang, L., Zhang, Y.,Shao, P. (2010). *Cancer Therapy Based on Nanomaterials and Nanocarrier Systems*. Journal of Nanomaterials 2010: 1-9.

Reddy, L. H., Dubernet, C., Mouelhi, S. L., Marque, P. E., Desmaele, D.,Couvreur, P. (2007). *A new nanomedicine of gemcitabine displays enhanced anticancer activity in sensitive and resistant leukemia types*. Journal of Controlled Release 124(1–2): 20-27.

Rinaudo, M. (2008). *Main properties and current applications of some polysaccharides as biomaterials*. Polymer International 57(3): 397-430.

Saravanakumar, G., Min, K. H., Min, D. S., Kim, A. Y., Lee, C. M., Cho, Y. W., Lee, S. C., Kim, K., Jeong, S. Y., Park, K., Park, J. H.,Kwon, I. C. (2009). *Hydrotropic oligomer-conjugated glycol chitosan as a carrier of paclitaxel: synthesis, characterization, and in vivo biodistribution*. J Control Release 140(3): 210-217.

Shi, D., Bedford, N. M.,Cho, H. S. (2011). *Engineered multifunctional nanocarriers for cancer diagnosis and therapeutics*. Small 7(18): 2549-2567.

Singh, R.,Lillard, J. W., Jr. (2009). *Nanoparticle-based targeted drug delivery*. Exp Mol Pathol 86(3): 215-223.

Sinha, R., Kim, G. J., Nie, S.,Shin, D. M. (2006). *Nanotechnology in cancer therapeutics: bioconjugated nanoparticles for drug delivery*. Mol Cancer Ther 5(8): 1909-1917.

Sinha, V. R.,Kumria, R. (2001). *Polysaccharides in colon-specific drug delivery*. Int J Pharm 224: 19-38.

Sloat, B. R., Sandoval, M. A., Li, D., Chung, W.-G., Lansakara-P, D. S. P., Proteau, P. J., Kiguchi, K., DiGiovanni, J.,Cui, Z. (2011). *In vitro and in vivo anti-tumor activities of a gemcitabine derivative carried by nanoparticles*. Int J Pharm 409(1–2): 278-288.

Son, Y. J., Jang, J. S., Cho, Y. W., Chung, H., Park, R. W., Kwon, I. C., Kim, I. S., Park, J. Y., Seo, S. B.,Park, C. R. (2003). *Biodistribution and anti-tumor*

efficacy of doxorubicin loaded glycol-chitosan nanoaggregates by EPR effect. Journal of Controlled Release 91(1-2): 135-145.

Stella, B., Arpicco, S., Rocco, F., Marsaud, V., Renoir, J. M., Cattel, L.,Couvreur, P. (2007). *Encapsulation of gemcitabine lipophilic derivatives into polycyanoacrylate nanospheres and nanocapsules*. Int J Pharm 344(1-2): 71-77.

Trickler, W. J., Khurana, J., Nagvekar, A. A.,Dash, A. K. (2010). *Chitosan and glyceryl monooleate nanostructures containing gemcitabine: potential delivery system for pancreatic cancer treatment*. AAPS PharmSciTech 11(1): 392-401.

Wang, B., Wang, L.-j., Li, D., Adhikari, B.,Shi, J. (2011). *Effect of gum Arabic on stability of oil-in-water emulsion stabilized by flaxseed and soybean protein*. Carbohydrate Polymers 86(1): 343-351.

Wang, C. X., Huang, L. S., Hou, L. B., Jiang, L., Yan, Z. T., Wang, Y. L.,Chen, Z. L. (2009). *Antitumor effects of polysorbate-80 coated gemcitabine polybutylcyanoacrylate nanoparticles in vitro and its pharmacodynamics in vivo on C6 glioma cells of a brain tumor model*. Brain research 1261: 91-99.

Wilson, B., Samanta, M. K., Santhi, K., Kumar, K. P., Ramasamy, M.,Suresh, B. (2010). *Chitosan nanoparticles as a new delivery system for the anti-Alzheimer drug tacrine*. Nanomedicine 6(1): 144-152.

Wu, Y., Yang, W., Wang, C., Hu, J.,Fu, S. (2005). *Chitosan nanoparticles as a novel delivery system for ammonium glycyrrhizinate*. Int J Pharm 295(1–2): 235-245.

Xu, Y.,Du, Y. (2003). *Effect of molecular structure of chitosan on protein delivery properties of chitosan nanoparticles*. Int J Pharm 250(1): 215-226.

Yang, Y.-Y., Wang, Y., Powell, R.,Chan, P. (2006). <*Polymeric core-shell nanoparticles for therapeutics*. Clinical and Experimental Pharmacology and Physiology 33: 557-562.

Ye, A., Flanagan, J.,Singh, H. (2006). *Formation of stable nanoparticles via electrostatic complexation between sodium caseinate and gum arabic*. Biopolymers 82(2): 121-133.

Yoo, H. S., Lee, J. E., Chung, H., Kwon, I. C.,Jeong, S. Y. (2005). *Self-assembled nanoparticles containing hydrophobically modified glycol chitosan for gene delivery*. J Control Release 103(1): 235-243.

You, J., Hu, F. Q., Du, Y. Z.,Yuan, H. (2007). *Polymeric micelles with glycolipif-like structure and multiple hydrophobic domains for mediating molecular target delivery of paclitaxel*. Biomacromolecules 8: 2450-2456.

Zhang, H., Ma, Y.,Sun, X. L. (2010). *Recent developments in carbohydrate-decorated targeted drug/gene delivery*. Med Res Rev 30(2): 270-289.

Zhang, J., Chen, X. G., Li, Y. Y.,Liu, C. S. (2007). *Self-assembled nanoparticles based on hydrophobically modified chitosan as carriers for doxorubicin*. Nanomedicine 3(4): 258-265.

8 Appendix

A – Gemcitabine calibration curves

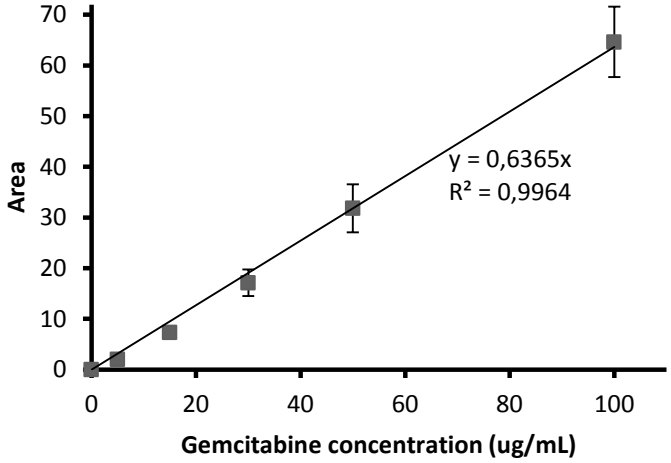

Figure 14 – Gemcitabine calibration curve in water. Data represented as mean ± SD (n = 3).

$$y = (0.6365 \pm 0.0127)x$$

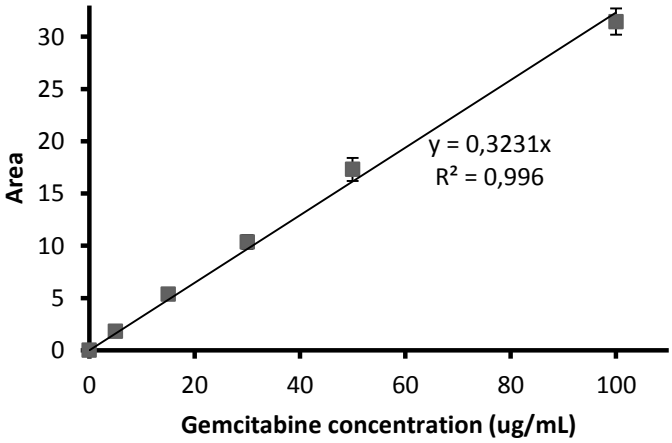

Figure 15 – Gemcitabine calibration curve in PBS at pH 7.4. Data represented as mean ± SD (n = 3).

$$y = (0.3231 \pm 0.0064)x$$